Petrological characterisation of magma storage

Teresa Ubide[1]*, Penny Wieser[2], Olivier Bachmann[3], Guil Gualda[4], David A. Neave[5], Pablo Samaniego[6], Adam Kent[7]

1. School of the Environment, The University of Queensland
2. Department of Earth and Planetary Science, University of California, Berkeley
3. Department of Earth and Planetary Sciences, ETH Zurich
4. Earth & Environmental Sciences, Vanderbilt University
5. Department of Earth and Environmental Sciences, University of Manchester
6. Laboratoire Magmas et Volcans, Université Clermont Auvergne-CNRS-IRD
7. College of Earth, Ocean and Atmospheric Sciences, Oregon State University

**corresponding author:*
t.ubide@uq.edu.au
https://www.linkedin.com/in/teresa-ubide-a17a17183

Peer-reviewed chapter submitted to *EarthArXiv*, accepted for publication in:
The Encyclopedia of Volcanoes, 3rd Edition
Eds: Bonadonna, Caricchi, et al. Elsevier
Chapter 4.2 within Part 1: Tectonics and magmatic plumbing systems

Abstract
Magma storage modulates the explosivity, frequency, and impact of volcanic eruptions, and controls the formation of magmatic-hydrothermal mineral deposits. The architecture of magma storage and plumbing systems, and their eruption triggering mechanisms, are inaccessible to direct observation in active volcanoes. However, they can be accessed through the study of products of volcanic eruptions: volcanic rocks and the crystal, melt, and gas records they contain. This chapter explores the texture and composition of volcanic rocks (and their plutonic cargoes) to better understand pre-eruptive magma storage and transfer from storage to eruption. We take a rock-centred approach to understanding magma-mush storage systems feeding volcanism, discussing traditional as well as new approaches, and their implications for volcano monitoring efforts.

Keywords
magma, crystal, mineral, zoning, melt inclusion, fluid inclusion, rock, experimental petrology, geochemistry, microanalysis, thermobarometry, petrography, thermodynamic modelling, thermomechanical modelling, plumbing system

Glossary (to be merged with other Part 1 ‘Tectonics and magmatic plumbing systems’ chapter glossaries)

- Crystal cargo: collective term for all the crystals in an erupted sample.
- Megacryst: very large magmatic crystals, typically >1 cm.
- Phenocryst or macrocryst: large magmatic crystals that are obvious to the naked eye (non-genetic term used to describe crystals that are notably larger than the surrounding matrix, irrespective of their origin).

- Microcryst: small crystals that constitute the groundmass or matrix of a volcanic rock or are notably smaller than phenocrysts/macrocrysts (non-genetic term used to describe small crystals within the rock matrix).
- Microlite: microcrysts with a high aspect ratio due to rapid crystallisation at high degrees of magma undercooling during magma ascent and eruption, typically <30 μm in width and <1/3 in width/length aspect ratio.
- Matrix or groundmass: fine-grained portion of the volcanic rock that represents the final erupted melt (or liquid), which often carries a cargo of large crystals from depth. The matrix or groundmass can be holocrystalline (composed of microcrysts), hypocrystalline (microcrysts and glass), or completely glassy.
- Autocryst: crystal composition in equilibrium with the host magmatic liquid. The term refers to chemistry and can refer to an entire crystal or to a zone of a crystal.
- Antecryst: crystal composition that is not in equilibrium with the host magmatic liquid (from a major, trace element, or isotopic perspective), recording crystallisation from earlier melts in the magmatic system. The term refers to chemistry and can refer to an entire crystal or to a zone of a crystal.
- Xenocryst: crystal composition foreign to the magmatic system, including material incorporated from the mantle or crust during magma ascent. The term refers to chemistry and can refer to an entire crystal or to a zone of a crystal.
- Crystal zoning: variation in the chemistry of a crystal as it grows.
- Concentric zoning: coherent chemical variations in a magmatic crystal from core to rim. Normal zoning reflects magma cooling and crystallisation with more primitive compositions in the interior to more evolved in the exterior, for example when anorthite in plagioclase decreases from core to rim. In contrast, reverse zoning (e.g., a marked jump to higher anorthite in plagioclase) suggests a temperature increase that may be associated with mafic magma recharge and mixing.
- Oscillatory zoning: cyclic chemical variations in a magmatic crystal from core to rim,
- Sector zoning: chemical variations in a magmatic crystal that follow crystallographic orientation, such as hourglass sector zoning where sectors grown along different crystallographic orientations have different compositions.
- Melt inclusion: parcel of melt trapped into a magmatic crystal as it grows.
- Fluid inclusion: parcel of exsolved fluid trapped into a magmatic crystal as it grows or is later fractured.

Introduction

The start, evolution and end of volcanic eruptions are closely linked to the way magma is stored beneath the Earth's surface and transported to eruption through magma plumbing systems. Magma storage also affects the magnitude, explosivity and frequency of eruptions, and the lifetime of volcanic systems. This chapter provides an overview on how we can investigate magma storage using the petrology of erupted products. Information derived from erupted materials, including rock and mineral textures and compositions, and melt and fluid inclusions, can be used to journey beneath a volcano, to better understand how and where magmas are stored and why they become remobilised in the lead-up to eruption (Fig. 1). We will take a rock-centred perspective into magmatic processes, discussing traditional and innovative approaches and implications for the monitoring of active volcanoes and the ways that volcanic eruptions are initiated. We summarise approaches to constrain storage

conditions in a How-to Box, and we use Case study Boxes and figures to highlight key volcanic systems that have guided our understanding of magma storage.

From generation in the Earth's mantle to eruption at the surface, magmas can stall and evolve in multiple storage regions within the lithosphere, with tectonic settings and magma productivity imposing a first order control on magmatic architecture and composition (Fig. 2). Convergent margins generate arc magmatism where thickened crust (particularly in continental arcs) and high magmatic water contents lead to storage in multi-level reservoirs that may span the thickness of the crust [1]. Enhanced cooling and differentiation in the shallow crust promote magma evolution and the potential for explosive volcanism through accompanying increases in viscosity and volatile contents (cf. chapter 2.2.1). Mid-ocean ridges represent the other end-member context (cf. chapter 2.2.3), involving shallow melt generation from relatively dry, decompressed mantle and comparatively modest differentiation en-route to the surface – with magma supply and melt fraction increasing with spreading rate [2]. Hotspot volcanoes vary widely depending on the thickness of the overlying plate and the degree of magma flux (cf. chapter 2.2.2). In ocean island basalts with low magma flux (e.g., Canary Islands, Cape Verde), eruptions can be primarily fed from upper mantle reservoirs with limited crustal storage [3]. Occasionally, the growth of shallow storage regions may lead to eruption of magma with more evolved compositions, including large ignimbrites. In contrast, high-flux settings like Hawaii or Réunion develop stable shallow storage regions where continued basaltic magma supply feeds high frequency mafic volcanism [4] (Fig. 2). In continental hotspots (e.g., Yellowstone, Snake River Plain, East Australia), crustal thickness imposes complexities additional to magma flux. Finally, other regions of high magma production include areas of local extension (e.g., Taupō Volcanic Zone and Long Valley calderas).

Petrological constraints provide complementary information to geophysical evidence (cf. chapter 1.4.1) highlighting that magma reservoirs are often mushy (Fig. 2), dominated by crystals (>50-60 vol.%) that record complex interactions between resident and replenishing magmas. In addition, unlike geophysical data providing an image of the current state of a volcanic plumbing system, the petrological study of earlier eruptions helps us build the history of processes modulating the magmatic system through time. Accumulation of eruptible magma, which requires enough liquid to allow ascent to the surface to erupt, is often transient [5] and understanding the switch from dormancy to eruption requires detailed petrological investigation. Refined constraints on the anatomy of magma plumbing systems, including the size, location, connectivity and eruptible melt fraction of magma reservoirs are essential for informing eruption forecasting across countries with varied resources and volcano awareness. Thus, petrological characterisation of active magmatic systems contributes to volcano preparedness into the future, supporting an important societal goal: to reduce the adverse effects of natural disasters on people and the economy (United Nations Sustainable Development Goal #11, Target 11.5). In addition, accurate constraints on magma storage are key to better understand the formation of magmatic-hydrothermal deposits of critical metals like lithium or copper in magmatic arcs, or rare earth elements in alkaline settings, leading to improved exploration strategies and increased discovery rates to meet the fast growing demand for the metals of the future (Goal #7: Affordable and clean energy; cf. chapters in part 8).

Deconstructing volcanic rocks

Magmas are complex multiphase mixtures composed of **liquid** (melt), **solid** (crystals) and **exsolved volatiles** (gas, liquids or supercritical fluids depending on compositions and pressure-temperature conditions) that may or may not be in equilibrium with one another. Erupted rocks are frozen versions of the magmas that reach the surface, where different components record distinct magmatic journeys from their source to eruption (Fig. 1). Therefore, volcanic rocks hold clues to magma storage and ascent that can be unveiled through the study of rock textures and compositions (Fig. 3). Accessing this information may be challenging, but different materials and spatial scales provide varying insights. At the first order, the major and trace element and isotope compositions of bulk rock samples and glasses (quenched liquids) provide information on source characteristics, partial melting and differentiation processes. Compositional and textural information from individual crystals and smaller parts thereof – including melt and fluid inclusions – provide greater insight into the intricacies of pre-eruptive magma storage. Analyses of rocks and mineral components sequentially erupted from a single volcano or a volcanic province can reveal temporal changes in source and differentiation processes at different time scales and through different ascent pathways. We explore these ideas in the following text and in the examples provided in Fig. 4-5 and as Case study Boxes.

Different crystal types provide access to different portions of the magma storage and ascent history. Phenocrysts (or macrocrysts) are large crystals formed in magma reservoirs during relatively long timescales of crystal growth compared to small microcrysts in the surrounding matrix, including microlites which crystallise rapidly upon ascent through the shallow conduits, as well as during eruption and emplacement (Fig. 1). Phenocrysts may therefore record long-term variations in magma storage conditions though their textures and compositions (Fig. 3-5). The phenocryst assemblage found in a single sample can represent diverse origins and residence times because different minerals may crystallise from magmas of different compositions and at different pressures, temperatures, oxidation states and volatile contents (i.e., magmatic environments)(Fig. 5). In many volcanic rocks, different batches of magma may often be mixed together, and thus all the crystals present in an erupted sample – often denoted as the crystal cargo – may be complex and have compositions that are not in chemical equilibrium with the erupted liquid fraction or with other crystals [6, 7]. Such populations are often described as antecrysts (when the crystal composition is genetically related to the volcanic system but not the specific eruption, like early cores recycled from more primitive or more evolved batches of melt) or xenocrysts (when the mineral composition is foreign to the magmatic system, as is the case of material incorporated from the crust or mantle). Mineral compositions in equilibrium with the host magmatic liquid may represent only a small fraction of the phenocryst material and can be distinctively referred to as autocrysts. Complex magma histories also commonly lead to individual crystals consisting of a combination of antecrystic, xenocrystic, and autocrystic zones.

Concentric or other forms of compositional zoning in crystals can reflect progressive changes in the magmatic environment during magma storage, particularly when the compositional change is strong and/or associated with a textural change. Examples of reverse zoning – consisting of rims of mafic composition including forsterite-rich olivine, Mg-Cr-rich clinopyroxene, or anorthite-rich plagioclase overgrowing earlier cores that may show

partially dissolved textures – are common indicators of replenishment of the stored magma with notably more primitive magma (e.g., [6, 7]). This is an important observation because many eruptions are triggered by mafic recharge and subsequent mixing [8] (cf. chapter 1.5.1). In contrast, low amplitude euhedral oscillations involving limited compositional change (e.g., small variations in anorthite in oscillatory zoned plagioclase) can be related to minor fluctuations in temperature, volatile content or growth kinetics without involving new melt, or to successive replenishment of stored magma with new magma of more similar composition. Storage of compositionally variable crystals at high temperature induces diffusive relaxation of compositional contrasts, which develops at distinct rates for different elements in different minerals at different temperatures. Diffusion modulates the preservation of zoning patterns (Fig. 5) but also enables calculation of the timescales of magmatic processes (e.g., [5]; cf. chapter 1.4.3).

Crystal textures also contain important information. The rate at which crystals grow determines crystal sizes, morphologies and certain zoning styles. Growth rate is linked to the degree of supersaturation, often represented by the degree of magma undercooling (ΔT), which measures the difference between the saturation temperature and the temperature of the magma: $\Delta T = T_{liquidus} - T_{crystallisation}$ [9]. Undercooling is an essential driver of crystallisation, and it increases if the temperature of the magma decreases (via cooling) or if the liquidus temperature increases (e.g., via degassing). The degree of undercooling is particularly high upon magma ascent and eruption, as magma is subjected to decompression-driven degassing conditioning the abundance, size, shape and distribution of microlites in the erupted rock matrix (Fig. 1), which can be used to calculate ascent rates (cf. chapters 1.4.3 and 1.5.2). In contrast, low undercooling imposes sluggish nucleation, which promotes the growth of phenocrysts. Common magma dynamics including recharge, mixing, convection and transfer impose low to moderate degrees of undercooling that can lead to growth of phenocrysts with skeletal morphologies (e.g., olivine [10]) or sector zoning, where sectors grown along different crystallographic orientations have different compositions despite forming coevally from the same bulk melt (e.g., hourglass sector zoning in clinopyroxene [11]). The style and degree of crystal zoning can therefore be exploited to investigate dynamic magma histories (Fig. 5).

As they grow, crystals may trap droplets of melt and exsolved fluid or vapour (melt and fluid inclusions; chapter 1.2.2), providing insights into the composition of these phases in the magmatic system at the time of entrapment (Fig. 1, 3). Melt inclusions trapped in minerals of different phases (e.g., olivine, pyroxene, plagioclase, quartz) and different compositions during prolonged storage can provide insight into mantle source variations, magma mixing events, fractional crystallisation, and the timing of volatile exsolution. Some melt and fluid inclusions are also trapped during ascent to the surface, particularly in H_2O-rich systems where degassing leads to increased undercooling and a burst of crystallisation upon ascent, which also impacts magma rheology (cf. chapter 1.2.3). During and after trapping, melt and fluid inclusions can be subject to a range of syn- and post-eruptive processes, and these can mask variations in melt and fluid compositions present at the time of trapping. Assessing these requires careful evaluation of data, often in concert with laboratory reheating and homogenisation or numerical correction [12].

The erupted rock matrix (or groundmass) represents the final magmatic liquid reaching the Earth's surface and is chemically distinct from the bulk rock in phenocryst-rich (porphyritic)

samples. The matrix can be microcrystalline to glassy depending on cooling rate upon ascent and eruption, and on the initial melt volatile contents: matrix in tephra (fast cooling or fast ascent) is more commonly glassy than in lava flows (slow cooling or slow ascent), and dryer magmas are more likely to quench to glass than wetter magmas, which undergo extensive crystallisation of plagioclase microlites upon degassing. The matrix represents magmatic liquid that has typically undergone mixing and homogenisation and may have optimal physical properties for eruption, which contrasts with melt inclusion records which can trap a range of heterogeneous melts entering, or remaining in, the system during storage [13, 14]. In addition, the matrix record is more extensively degassed than the melt inclusions, because it has re-equilibrated at low pressure (chapter 1.2.2). We note, however, that matrix in rapidly quenched samples, or those erupted underwater, can still retain high volatile contents because of incomplete diffusion of volatile elements and limited degassing due to the overlying water pressure. Hence, melt inclusion and matrix compositions provide records of stored vs. erupted liquids respectively, and enable reconstruction of a range of magmatic processes from source melting to differentiation mechanisms and eruption triggers.

Magma storage and architecture

Volcanoes are the tips of large magmatic systems that extend from their source, typically located in the Earth's mantle, to the surface. Within these complex and vertically extensive magma plumbing systems, magmas may get trapped and differentiate into more evolved compositions (Fig. 2). Magmas may preferentially stall at rheological, density, and other discontinuities like the crust-mantle boundary and the brittle-ductile transition in the shallow crust, as well as along key levels of volatile saturation and degassing-induced crystallisation where magma viscosity increases (Fig. 5; cf. chapter 1.2.3). Constraining the depths at which magmas are stored before eruption, as well as the temperature, chemical composition, oxidation state, crystal and volatile content of magma reservoirs, their connectivity and ascent pathways to eruption, allows the reconstruction of the anatomy of plumbing systems, essential for interpreting signals of volcanic unrest (e.g., Case study Boxes).

The depth and vertical extent of storage regions are some of the most valuable constraints on magmatic architecture. Petrological constraints on storage depth (How-to Box) can be combined with seismicity and ground deformation in the monitoring of active volcanoes. In addition, storage depth places first order controls on the fractionating mineral assemblage (e.g., Fig. 5) and therefore the chemical evolution of magma, which in turn influences the potential for explosive volcanism, economic mineralisation and crustal growth. Noting that most petrological methods reconstruct pressure rather than depth directly, these pressures must be converted into storage depths following assumptions about the crustal and mantle density profile beneath the volcano.

Pressure (P), temperature (T) and other intensive parameters independent of system size (e.g., oxidation state, magma and melt compositions, and volatile concentrations) can be calculated from mineral, melt and volatile compositions using a wide variety of empirical and thermodynamic models (How-to Box; e.g., Fig. 4). These models are calibrated with experimental petrology data, by measuring the products of laboratory experiments in which

magmas have been equilibrated at different conditions. For example, clinopyroxene-melt barometers relating the exchange of the Na-rich jadeite component between clinopyroxene and melt have been developed by combining experiments conducted at a wide range of pressures and temperatures with thermodynamic data on the change in volume of crystallised clinopyroxene [15]. Similarly, extensive experimental work has determined how the solubility of H_2O and CO_2 in silicate melts is related to pressure (as well as temperature, and melt composition), forming the basis of melt inclusion barometry where measured volatile contents are converted into pressures. Further, experimental constraints on the equation of state of CO_2 ($\pm H_2O$), which parameterises how pressure, temperature and density relate to each other, are used to calculate the pressure at which fluid inclusions were trapped or re-equilibrated from a measured CO_2 density and an estimate of entrapment temperature [16]. In silicic magmas, amphibole barometry has often been used to assess crystallisation depths and, more recently, barometry using only melt compositions has opened new perspectives in the reconstruction of magma architecture ([17] and further reading website list).

Thermometers provide further key information that helps us identify the number of different magmatic environments contributing towards any given erupted magma, as well as to track the role of mafic recharge in triggering magma mixing, ascent and eruption. The erupted melt composition, particularly in systems with a small number of phases, typically holds most substantial temperature information. A range of minerals also have compositions sensitive to temperature from mafic (e.g., olivine, pyroxenes) to intermediate (e.g., plagioclase, amphibole) to felsic magmas (e.g., Ti-in-zircon and -quartz, Fe-Ti oxides magnetite-ilmenite) and can be exploited to calculate magmatic temperatures. Additional storage conditions include f_{O2} (oxygen fugacity, which measures the redox state of the magma, often determined from reactions sensitive to the Fe^{2+} and Fe^{3+} contents of different phases), as well as volatile contents (H_2O, CO_2, both dissolved and exsolved, as well as other volatile elements such as S, halogens including F and Cl, and noble gases; cf. chapter 1.2.2). Constraining these parameters is fundamental for reconstructing ore formation processes (e.g., copper porphyry deposits) and growth rates of magma reservoirs, predicting eruptive styles, and understanding the abundance and speciation of volcanic gas emissions.

Combining diverse approaches can increasingly overcome the large uncertainties traditionally associated with petrological calibrations (How-to Box). Many of these uncertainties are associated with historical limitations in analytical precision, the scope of experimental datasets used for calibration, the limited pressure sensitivity of many mineral-melt reactions [16] and, importantly, challenges in identifying equilibrium assemblages in natural samples. Experimental calibrations often use mineral-melt or mineral-mineral equilibrium pairs, and the achievement of equilibrium needs to be tested on the natural dataset before constraints on intensive parameters can be retrieved by applying experimentally derived calibrations. For example, mineral-melt thermobarometry requires pairing mineral compositions with liquid compositions with which they equilibrated. A reasonable approach is to pair crystal cores with melt inclusions (after correcting for post-entrapment crystallisation) and crystal mantles or rims with matrix or glass compositions; then, thermobarometric calculations are applied only to equilibrium pairs (e.g., [18] and additional online references for testing clinopyroxene-melt equilibrium). Additionally, natural compositions should fall within the compositional bounds of the experimental calibration datasets. In line with this, new machine learning approaches can boost quantification of

intensive parameters by identifying the experimental mineral compositions that best match the natural compositions of interest (e.g., [19]). These approaches are not yet based on thermodynamic principles and in some case provide results that deviate from traditional thermobarometry (noting that different traditional thermobarometers may also differ from one another). This discrepancy highlights the need to critically compare thermodynamic- and machine learning-based models to identify potential issues, re-evaluate calibration datasets, and move towards the development of hybrid models based on thermodynamics and machine learning. Testing a range of thermobarometric models appropriate for the system of interest and accounting for uncertainties when examining the statistical distribution of results is now substantially eased by new open-source tools (e.g., [19], [20]), and multi-method thermobarometry holds promise for better quantifying magma storage conditions.

An additional, complementary approach to estimate storage conditions is to forward model liquid and mineral chemistries during differentiation of a given starting composition at varying pressure, temperature, oxidation state and water contents, using thermodynamic packages that consider experimental phase equilibria and mineral thermodynamic models (How-to Box). Modelled predictions can be compared to measured data in natural samples to assess likely conditions of magma storage and evolution (Fig. 4). This includes the chemical evolution of the magmatic liquid at given conditions, as well as the stability of mineral phases and their compositions, from a wide spectrum of mafic to felsic magmas (e.g., using the program rhyolite-MELTS [21] and other thermodynamic models, cf. How-to Box and further reading website list). For instance, modelling the depth, temperature, magmatic water content and oxidation state that control zircon saturation from felsic magma compositions can help interpret the thermal, geochronological and trace element information obtained independently from zircon in the system. Further, thermodynamic models allow estimation of physical parameters such as sensible and latent heat loss during solidification, which are difficult to obtain using other methods. Ongoing efforts to optimise thermodynamic modelling include expanding the modelling of phase equilibria in complex mineral phases (e.g., amphiboles) and exotic magma compositions, such as highly alkaline magmas that can lead to enrichment in rare earth elements, as well as incorporating trace elements and isotope ratios into models. Constraints from thermodynamic models do not always agree with other petrological methods, and contrasting results can steer fundamental discussions on the conditions of magma storage (e.g., Bishop Tuff; Fig. 4 and Case study Box 2). Thermodynamic models can help quantify additional intensive and extensive properties such as melt and fluid fraction, density and viscosity that can be used to investigate how magma is stored at given conditions, and why it may be primed to erupt, as we explore below.

Magma dynamics and differentiation

Dynamic processes within magma storage regions exert a strong control on the potential for volcanic eruption at the surface, and on the type and evolution of volcanic activity. During the active period of source-to-surface differentiation columns (Fig. 2), many magmas remain as mushes, i.e., zones of melt with crystal contents high enough (>50-60 vol.%) that they are largely locked and immobile. Mush zones can also contain a significant fraction of exsolved volatiles, particularly in the upper crust. Mushes are seen as the main sites of chemical differentiation, where separation of crystals, melts and volatiles can happen through a variety of processes including hindered settling, crystal repacking and viscous compaction [22].

Such phase separation leads to melt accumulation at certain levels of differentiation columns, and crystal accumulation (cumulates) in others, while volatiles feed shallow ore deposits and are ultimately released to the atmosphere.

Across tectonic settings, distinct magma generation conditions impose primary controls on the major and trace element and isotopic evolution of magmas, their volatile budgets, magmatic architecture and eruption triggering mechanisms (Fig. 2). Arc settings typically generate hydrous, oxidised magmas where fractionation involves hydrated minerals like amphibole and biotite, in addition to clino- and orthopyroxene, magnetite and ilmenite, and a boost in plagioclase crystallisation upon shallow degassing. In contrast, magma evolution in dry mid-ocean ridges and hotspots follows simpler evolutionary paths dominated by variable fractionation of olivine, pyroxene, plagioclase and Fe-Ti oxides. In settings where low degrees of melting of enriched sources generate strongly alkaline, silica-undersaturated magmas, magma evolution may involve saturation of feldspathoids including leucite or nepheline. Within a given magma suite, pressure imposes key stability constraints on the crystallising assemblage, as discussed above and illustrated in Fig. 5. Storage conditions become increasingly challenging to decode with increasing pressure, as deep mush components are less likely to reach the surface. However, deep magma evolution may be as important as it is cryptic. For example, deep garnet fractionation in thick continental arcs may lead to rare earth element fractionation and magma oxidation that may increase porphyry copper fertility once the magma reaches shallow depths (e.g., [23]).

The complexity of magma storage regions, and their incremental growth over long periods of time, mean that magma differentiation rarely follows closed-system evolution of continuous cooling leading to equilibrium or fractional crystallisation and normal zoning in autocrystic minerals. Isotopic evidence and crystal archives in volcanic rocks commonly indicate open-system evolution with repeated replenishment and mixing of distinct magma batches as well as crustal assimilation, developing disequilibrium textures and compositional changes as crystals grow (petrological cannibalism and antecrysts recycling; Fig. 5). Textural features in minerals such as sieve textures are commonly linked to rapid dissolution and recrystallisation associated with mafic recharge and mixing. Alternatively, they can record water loss or flushing from deeper reservoirs, particularly of less soluble CO_2-rich fluid. This is because increasing the proportion of CO_2 in the fluid phase results in a drop in the solubility of H_2O in the co-existing melt, and thus H_2O degassing [6].

The degree of disequilibrium can be assessed using textural observations together with major, trace element and isotope data at scales ranging from bulk rock to individual crystal zones and melt inclusions. At the melt scale, closed-system fractional crystallisation generates liquid lines of descent in bivariate plots of major element oxides or trace element compositions against a differentiation index such as increasing SiO_2 or decreasing MgO. In these liquid lines of descent, changes in the fractionating assemblage generate kinks in the patterns, such as a drop in Fe and Ti when Fe-Ti oxides join the assemblage. In contrast, open-system processes including episodes of magma recharge, mixing, crustal assimilation or crystal accumulation make natural compositions deviate from the closed-system evolution, typically resulting in straight mixing lines between two or more compositional end-members. At the mineral scale, closed-system evolution generates coherent compositional trends in bivariate plots against differentiation indices such as decreasing anorthite in plagioclase, forsterite in olivine or Mg-number in pyroxene. Small variations along the

evolutionary trend may be induced by kinetic effects like sector or fine-oscillatory zoning, whereas inherited antecrysts or xenocryst cores typically deviate from the main trend. Assessing the genetic links amongst crystal populations benefits from combining major element data with trace element concentrations and ratios, and isotope ratios.

Mush complexities can also be more cryptic. For example, recharging magmas may react with the existing crystal mush, resulting in melt and mineral compositions that cannot be explained by fractional crystallisation alone. Reactive flow is a plausible differentiation mechanism in mush reservoirs and it has been widely documented, particularly below mid-ocean ridges [24]. Increasing resolution and precision of petrological data and thermodynamic modelling can progressively untangle the history of processes across magmatic systems, and how they modulate magma evolution.

Interrupting storage. Ascent to eruption and impact on the rock record

Magma recharge and mixing in storage regions can trigger eruptions across tectonic settings. Mixing introduces changes in magma chemistry, temperature, volatile content, density and viscosity that can lead to increased magma buoyancy and overpressurisation in the reservoir, triggering mush remobilisation and magma ascent (cf. chapter 1.5.2). The chemical and physical state of resident and recharge magmas are important determining factors, and not all recharge events lead to eruption (cf. chapter 1.5.1), contributing instead to growth of the magma reservoir. Crucially, the fact that some magmas are more eruptible than others means that some volcanic records may be inherently biased, particularly towards mixed (intermediate) compositions [14]. Mixing can homogenise magmas sourced from compositionally heterogenous mantle sources upon storage and ascent to eruption. Yet, individual eruptions may sample heterogeneities on timescales of weeks to months to years, as recorded in specific volcanic systems and eruptions within Iceland [25], La Palma, or the Ecuadorian arc (cf. additional online references).

Despite filtering of eruptible melts through multi-level mushes, volcanic rocks have the great advantage of rapid quenching upon eruption, which means magmatic histories can be extracted from crystal, melt, and melt/fluid inclusion records, which may preserve heterogeneities before or during mixing events. Yet, volcanic rocks may only record the end point of a complex series of magmatic evolution, whilst plutonic rocks from exhumed crustal sections provide direct insight into volcanic plumbing systems. However, there are additional complexities associated with plutonic rocks. The plutonic environment enhances chemical diffusion and re-equilibration, which can blur or erase chemical histories. In addition, plutonic rocks may have a cumulate origin, which means that bulk rock compositions of plutonic rocks may not represent melt compositions. Further, many crystals form in near-solidus conditions, which can limit the preservation of identifiable magmatic histories. Moreover, juxtaposition of countless intrusive events over many millennia, which may or may not mix/mingle, lead to a complex plutonic puzzle that is challenging to assemble. Nevertheless, plutonic rocks may provide a more complete view of fossil magmatic reservoirs and their potential hydrothermal cap, which may become largely degassed in active volcanoes. Growing research stresses the need to integrate volcanic and plutonic research to better understand magma storage, as highlighted in the next section.

From mushes to plutons: the volcanic-plutonic connection

Distinguishing regions of melt accumulation vs. crystal accumulation in the plutonic roots of volcanoes remains a challenge, particularly for the upper, more silicic levels of differentiation columns, where crystal-melt separation is likely slower than in the deeper, hotter, less viscous, mafic reservoirs [22]. However, in recent decades different techniques have been developed to discriminate between melt vs. crystal accumulation, including geochemical and textural analyses. Cumulates of more evolved compositions are now being identified in all types of plutonic terrain, and as plutonic fragments or crystal-rich clasts in volcanic rocks (e.g., [26]).

Plutonic fragments (fragments of coarse-grained holocrystalline rock) or crystal-rich clasts (melt-bearing crystal-rich juvenile fragments) are common in volcanic rocks of varied compositions and settings. Such fragments or clasts can hold a textural record of the relative 'mushiness' of magma storage areas, including evidence of crystal accumulation, providing a link between the plutonic and volcanic realms. Crystals grown in liquid-dominated environments can move, become re-arranged by flowing melt, aggregate (synneusis), and settle, whereas crystals grown in crystal-dominated environments form in situ within the spatial and mechanical constraints of the mush. Thus, the quantification of crystal shapes, boundaries and junctions between crystals within mushy fragments, as originally developed on plutonic rocks, can provide insight into relative fractions of solid and liquid in storage regions, and their variations through time [27].

Broken plutonic fragments can become entrained into rapidly flowing magma and flushed to the surface, particularly towards the end of an eruption when reservoir drainage can result in wall-rock collapse. This explains the common occurrence of crystal-rich clasts and lithic xenoliths towards the end of explosive eruptions, and during the collapse event of caldera forming eruptions. In addition, evidence for mixing and mingling are ubiquitous in both the plutonic record (e.g., mafic microcrystalline enclaves, mafic-felsic composite dykes, crystal transfer) and the volcanic record (e.g., complex crystal populations and melt inclusion populations, mixed glasses, mafic enclaves). Recharge of new magma brings heat to shallower levels, allowing reheating and partial remelting of previously emplaced magmas that had cooled and crystallised. Hence, mush rejuvenation is a common process and can lead to remobilization or defrosting of material that would have otherwise been non-eruptible [26].

Despite the efficacy of mush remobilisation processes to drive eruptions, most magma in subvolcanic plumbing systems remains stuck in the crust, and never erupts. Hence, the extrusive/intrusive ratio, also referred to as the volcanic/plutonic ratio considering that the mush zones will ultimately turn into plutons, is typically << 1. Although a fundamental parameter of such crustal columns, this volcanic/plutonic ratio is poorly constrained, because it is hard to quantify and can vary in space and time due to different factors, including magma fluxes, composition, tectonic settings, as well as the mechanical properties of the multi-phase magmatic system and its crustal container. Ocean ridge settings (ophiolites) and rare, exposed sections of continental crust (e.g., [28]) provide ideal settings to investigate the intrusive to extrusive ratio. In addition, the use of thermomechanical models that consider the multi-phase nature of mush columns, as well as the rheological conditions

within and outside the mush zones, is fundamental to explore the complex evolution of storage systems (cf. chapter 1.5.3). In particular, understanding the growth of giant magma reservoirs that lead to supereruptions (some of the most destructive geological events our planet can produce) remains a great challenge for the volcanological community. Long-lived magmatic activity, leading to a thermally mature, more ductile crust plays a key role in making room for large reservoirs, and decreasing the volcanic/plutonic ratio to allow such reservoirs to grow (Fig. 2). In addition, other processes, like increased magma reservoir compressibility due to the presence of an exsolved gas phase, may also be important in generating these giant reservoirs [29].

Recent advances

The vertically extensive, commonly crystal-rich magma plumbing systems that underlie volcanoes we envision today (e.g., Fig. 2, 5) are much more complex than the relatively simple magma chamber models considered until only recently. Complexity in magmatic architecture and dynamics is increasingly unravelled by rapidly improving petrological techniques, including in situ analytical approaches that enable interpreting geochemical heterogeneities in a textural context (cf. examples in further reading website list). These include improved speed and quality of scanning electron microscopy (SEM) with back-scattered electron (BSE) and cathodoluminescence (CL) imaging, as well as mapping of major and minor elements with energy-dispersive X-ray spectroscopy (SEM-EDX) and synchrotron X-ray fluorescence microscopy (XFM). Innovations in high sensitivity quantitative analysis via electron probe microanalysis with wavelength-dispersive X-ray spectroscopy (EPMA-WDS) include the use of ultra-high resolution soft X-ray emission spectrometry (SXES), which allows measuring Fe valence state. At the trace element level, rapid mapping of a large range of elements at high spatial resolution is now routinely achievable via laser ablation inductively coupled plasma mass spectrometry (LA-ICP-MS; Fig. 5) and becoming increasingly faster with optimisations including time-of-flight (TOF) mass spectrometry. Further, elemental and isotopic variations can be resolved at ultra-high spatial resolution via secondary ion mass spectrometry (SIMS) and atom probe tomography (APT). Advancements in mass spectrometer sensitivity and the capability of data reduction packages increasingly allow routine measurement of isotope ratios in situ, such as Sr or U/Th/Pb/Hf isotopes via multi-collector (MC-)LA-ICP-MS. The laser approach makes it possible to rapidly resolve isotope variations across individual mineral zones, crystal populations and host melts, which allows assessing changes in the source and contamination of melts through time. While in situ analysis is less precise than traditional methods of analysis of bulk rock samples, mineral separates or micro-drilled material, the large volumes of data afforded by the speed and spatial resolution of these newer approaches make it possible to assess the consanguinity of melts involved in complex magma histories on statistically significant datasets.

For measurements of volatile species, advances in Raman spectroscopy in the last decade have allowed in situ, non-destructive measurements of pockets of CO_2 fluid down to ~1 µm. Analysis of CO_2-rich bubbles in melt inclusions has demonstrated that many magmas have an order of magnitude more CO_2 than was previously recognised. Raman analyses also allow measurements of fluid inclusions with a far wider range of densities and sizes than conventional microthermometry, where CO_2 densities are obtained by observing phase

changes, which is very difficult for inclusions trapped at <5 km depth, and for small inclusions <5-10 µm. Collectively, new developments improving precision and speed of volatile measurements are leading to an improved understanding of the concentration of volatiles in magmas, their entrapment pressure (depth), and their role in eruptive processes at many volcanoes globally.

The emerging view of highly complex pre-eruptive processes has increasingly highlighted the need to adapt experimental petrology approaches, which take significant time and effort to complete, to best reflect natural magmatic systems. Improving the ability to rationalise complexity in our observations of natural systems makes it possible to perform experiments under more complex, but still well-understood conditions. This involves optimising the design and analysis of equilibrium and kinetic experiments, so that they are more closely aligned with nature, particularly at relatively low pressures relevant to shallow crustal magma storage and transfer in the lead-up to eruptions. In addition, experimental run products are increasingly analysed with state-of-the art techniques that provide not only high spatial resolution and precision, but even temporal resolution when measurements are taken during the experimental run itself (e.g., 4D experimental petrology combined with fast synchrotron X-ray microtomography). Future research will also increasingly combine experiments with thermodynamic modelling. Combining both approaches in tandem remains largely unexplored and has strong potential to further quantify and test petrological hypotheses, driving petrological science forward.

Analytical techniques and petrological models have improved not only in resolution, accuracy and precision, but also in speed and automation, boosting the quantity of data used in petrological analysis, and therefore its statistical power and significance. The rapid increase in available geochemical and geochronological data has accelerated computational literacy in petrology. This includes open-source tools for processing data that increasingly include statistical and artificial intelligence approaches (cf. chapter 1.5.5), such as the identification of crystal populations with multi-dimensional image analysis and clustering of geochemical data. In addition, open data repositories that follow FAIR data principles (findable, accessible, interoperable, and reusable), such as GeoRoc, PetDB-EarthChem, or EarthBank (previously AusGeochem), allow mining large datasets to test petrological hypotheses on a global scale. We highlight the enduring importance of petrography (Fig. 1, 5) in underpinning new advances resulting from better analytical techniques, better models, and the growing maturation of quantification in the discipline. This will allow guiding petrological advancements as larger data and statistical methods are embraced, so that increasingly resolved, accurate and precise textural and chemical data continue to unveil petrological complexities during magma storage and transfer to eruption.

Links to multi-disciplinary volcano monitoring tools

Volcano monitoring efforts focus primarily on geophysical and geodetic information on seismicity and ground deformation, coupled with gas geochemistry. However, the petrology of juvenile erupted products (lava flows and tephra; Fig. 1) is the only means of gathering information on the magma dynamics and chemistry, which controls its physical properties (e.g., temperature, viscosity) and therefore hazard potential. Petrological studies have traditionally been time-consuming and volcano observatories have used petrology as a

forensic tool. But the last few years have seen dramatic improvements in petrological monitoring (cf. chapter 1.5.4), with near-real-time bulk rock analysis of lavas feeding emergency management in the 2018 eruption at Kīlauea, Hawaii and, since 2023, electron probe microanalysis results in Iceland getting not only to decision makers but also the public via social media within 24 h of eruption.

Recent eruptions where safe sampling could be undertaken during volcanic activity and combined with geophysical and gas monitoring information, such as the 2021 eruption at La Palma in the Canary Islands, permitted not only near-real-time petrological monitoring but also the development of petrological tools to use in future monitoring efforts. These include rapid Raman analysis of fluid inclusions to estimate depth of magma storage with high precision, combination of fluid inclusion microthermometry with seismicity to monitor magma ascent, and LA-ICP-MS analysis of volcanic matrix to monitor changes in the melt chemistry and their impact on eruptive style.

The largest challenge to petrological monitoring is to rapidly deliver increasingly high-quality data on a range of spatial scales to volcano observatories with variable resources. Volcano education and awareness in active regions is key to keep populations safe and to involve locals in the collection of samples where possible (cf. chapter 7.2.3). For example, early ash fallout can be invaluable to get primary textural and geochemical insight into the ensuing climactic eruption. Importantly, any real-time volcano monitoring is greatly facilitated by petrological work that reconstructs plumbing system architecture and typical eruption triggers (e.g., Fig. 4, 5). Petrological constraints are particularly valuable in systems where long periods of dormancy or low economic resources lead to limited volcano monitoring. Detailed petrological investigations of key past eruptions can be undertaken without the time pressure of an ongoing eruption, building our knowledge on the dynamics of magmatic systems and our frameworks for volcanic architecture, crucial for the interpretation of volcanic unrest and the evolution of eruptions.

Summary

Conceptual, experimental, numerical and analytical advances have meant the volcanological community can now interrogate the rock record to estimate the *what*, *where*, *how* and *why* of magma storage in different volcanic contexts. We encourage a petrography-led approach to explore magma storage at different scales, considering bulk to in situ chemical analyses of volcanic rock components, ranging from element to volatile concentrations to isotope ratios and their textural constraints. Together with experimental, thermodynamic, and thermomechanical constraints, the petrological community is increasingly unravelling magma storage linked to a range of tectonic settings, magma compositions and eruptive styles, contributing to improved monitoring of active volcanoes and their tipping mechanisms.

References

[1] Cashman KV, Sparks RSJ, Blundy JD (2017). Vertically extensive and unstable magmatic systems: A unified view of igneous processes. Science https://doi.org/10.1126/science.aag3055

[2] Coogan LA (2014). The lower oceanic crust. Treatise on Geochem, 2nd Ed. http://dx.doi.org/10.1016/B978-0-08-095975-7.00316-8

[3] Klügel A, Longpre MA, Garcia-Canada L, Stix J (2015). Deep intrusions, lateral magma transport and related uplift at ocean island volcanoes. Earth Planet Sci Lett 431, 140–149. https://doi.org/10.1016/j.epsl.2015.09.031

[4] Pietruszka AJ, Heaton DE, Marske JP, Garcia MO (2015). Two magma bodies beneath the summit of Kīlauea Volcano unveiled by isotopically distinct melt deliveries from the mantle. Earth and Planetary Science Letters 413, 90-100. https://doi.org/10.1016/j.epsl.2014.12.040

[5] Cooper KM, Kent AJR (2014). Rapid remobilization of magmatic crystals kept in cold storage. Nature 506, 480–483. https://doi.org/10.1038/nature12991

[6] Cashman K, Blundy J (2013). Petrological cannibalism: the chemical and textural consequences of incremental magma body growth. Contrib Mineral Petrol 166, 703–729. https://10.1007/s00410-013-0895-0

[7] Ubide T, Kamber BS (2018). Volcanic crystals as time capsules of eruption history. Nat Commun 9, 326. https://doi.org/10.1038/s41467-017-02274-w

[8] Sparks SRJ, Sigurdsson H, Wilson L (1977). Magma mixing: A mechanism for triggering acid explosive eruptions. Nature 267, 315–318. https://doi.org/10.1038/267315a0

[9] Hammer JE (2008). Experimental studies of the kinetics and energetics of magma crystallization. Rev Mineral Geochem 69, 9–59. https://doi.org/10.2138/rmg.2008.69.2

[10] Shea T, Hammer JE, Hellebrand E, Mourey AJ, Costa F, First EC, et al. (2019). Phosphorus and aluminum zoning in olivine; contrasting behavior of two nominally incompatible trace elements. Contrib Mineral Petrol 174, 1–24. https://doi.org/10.1007/s00410-019-1618-y

[11] Ubide T, Mollo S, Zhao JX, Nazzari M, Scarlato P (2019). Sector-zoned clinopyroxene as a recorder of magma history, eruption triggers, and ascent rates. Geochim Cosmochim Acta 251, 265-283. https://doi.org/10.1016/j.gca.2019.02.021

[12] Rose-Koga EF, Bouvier AS, Gaetani GA, Wallace PJ, Allison CM, Andrys JA, et al. (2021). Silicate melt inclusions in the new millennium; a review of recommended practices for preparation, analysis, and data presentation. Chem Geol 570, 120145. https://doi.org/10.1016/j.chemgeo.2021.120145

[13] Maclennan J (2008). Concurrent mixing and cooling of melts under Iceland. J Petrol 49, 1931–53. https://doi.org/10.1093/petrology/egn052

[14] Kent AJR, Darr C, Koleszar AM, Salisbury MJ, Cooper KM (2010). Preferential eruption of andesitic magmas through recharge filtering. Nature Geosci 3, 631–636. https://doi.org/10.1038/ngeo924

[15] Putirka KD (2008). Thermometers and Barometers for Volcanic Systems. Rev Mineral Geochem 69, 61-120. https://doi.org/10.2138/rmg.2008.69.3

[16] Wieser PE, Gleeson MLM, Matthews S, DeVitre C, Gazel E (2025). Determining the pressure–temperature–composition (PTX) conditions of magma storage. Treatise of Geochemistry (3rd edition) 2, 83-151. https://doi.org/10.1016/B978-0-323-99762-1.00024-3

[17] Gualda GAR, Gravley DM, Deering CD, Ghiorso MS (2019). Magma extraction pressures and the architecture of volcanic plumbing systems. Earth Planet Sci Lett 522, 118–24. https://doi.org/10.1016/j.epsl.2019.06.020

[18] Mollo S, Putirka K, Misiti V, Saligo M, Scarlato P (2013). A new test for equilibrium based on clinopyroxene–melt pairs: Clues on the solidification temperatures of Etnean alkaline melts at post-eruptive conditions. Chem Geol 352, 92-100. https://doi.org/10.1016/j.chemgeo.2013.05.026

[19] Ágreda-López M, Parodi A, Musu A, Jorgenson C, Carfi A, Mastrogiovanni F, Caricchi L, Perugini D, Petrelli M (2024). Enhancing machine learning thermobarometry for clinopyroxene-bearing magmas. Computers & Geosciences 193, 105707. https://doi.org/10.1016/j.cageo.2024.105707

[20] Wieser P, Petrelli M, Lubbers J, Wieser E, Ozaydin S, Kent A, Till C (2022). Thermobar: an open-source Python3 tool for thermobarometry and hygrometry. Volcanica 5, 349–384. https://doi.org/10.30909/vol.05.02.349384

[21] Gualda, GAR, Ghiorso, MS, Lemons, RV, Carley, TL (2012). Rhyolite-MELTS: A modified calibration of MELTS optimized for silica-rich, fluid-bearing magmatic systems. J Petrol 53, 875–890. https://doi.org/10.1093/petrology/egr080

[22] Bachmann O, Huber C (2019). The Inner Workings of Crustal Distillation Columns; the Physical Mechanisms and Rates Controlling Phase Separation in Silicic Magma Reservoirs. J Petrol 60, 3–18, https://doi.org/10.1093/petrology/egy103

[23] Lee CTA, Tang M (2020). How to make porphyry copper deposits. Earth Planet Sci Lett 529, 115868. https://doi.org/10.1016/j.epsl.2019.115868

[24] Lissenberg CJ, MacLeod CJ (2016). A reactive porous flow control on mid-ocean ridge magmatic evolution. J Petrol 57, 2195–2220. https://doi.org/10.1093/petrology/egw074

[25] Halldórsson SA, Marshall EW, Caracciolo A et al. (2022). Rapid shifting of a deep magmatic source at Fagradalsfjall volcano, Iceland. Nature 609, 529–534. https://doi.org/10.1038/s41586-022-04981-x

[26] Ellis BS, Wolff JA, Szymanowski D, Forni F, Cortes-Calderon EA, Bachmann O (2023). Cumulate recycling in igneous systems: The volcanic record. Lithos 456-457, 107284. https://doi.org/10.1016/j.lithos.2023.107284

[27] Holness MB, Stock MJ, Geist D (2019). Magma chambers versus mush zones: constraining the architecture of sub-volcanic plumbing systems from microstructural analysis of crystalline enclaves. Phil. Trans. R. Soc. A 377, 20180006. http://dx.doi.org/10.1098/rsta.2018.0006

[28] Miller CF, Furbish DJ, Walker BA, Claiborne LL, Koteas GC, Bleick HA, et al. (2011). Growth of plutons by incremental emplacement of sheets in crystal-rich host; evidence from Miocene intrusions of the Colorado River region, Nevada, USA. Tectonophysics 500, 65–77. https://doi.org/10.1016/j.tecto.2009.07.011

[29] Townsend M, Huber C, Degruyter W, Bachmann O (2019). Magma chamber growth during intercaldera periods: Insights from thermo-mechanical modeling with applications to Laguna del Maule, Campi Flegrei, Santorini, and Aso. Geochem Geophys Geosys 20, 1574–1591. https://doi.org/10.1029/2018GC008103

Further reading website list

Anderson AT, Davis AM, Lu FQ (2000). Evolution of Bishop Tuff rhyolitic magma based on melt and magnetite inclusions and zoned phenocrysts. J Petrol 41, 449–473. https://doi.org/10.1093/petrology/41.3.449

Arzilli F, Polacci M, La Spina G et al. (2022). Dendritic crystallization in hydrous basaltic magmas controls magma mobility within the Earth's crust. Nat Commun 13, 3354. https://doi.org/10.1038/s41467-022-30890-8

Bacon CR, Sisson TW, Mazdab FK (2009). Young cumulate complex beneath Veniaminof caldera, Aleutian arc, dated by zircon in erupted plutonic blocks. Geology 35, 491-494. https://doi.org/10.1130/G23446A.1

Barnes CG, Coint N, Yoshinobu A (2016). Crystal accumulation in a tilted arc batholith. Am Mineral 101, 1719-1734. https://doi.org/10.2138/am-2016-5404

Barnes CG, Werts K (2022). Magma Defrosting: Evidence from Plutonic Rocks. J Petrol 63(11), egac112. https://doi.org/10.1093/petrology/egac112

Barnes SJ, Paterson D, Ubide T, Schoneveld LE, Ryan C, Le Vaillant M (2020). Imaging trace-element zoning in pyroxenes using Synchrotron XRF mapping with the Maia detector array: benefit of low-incident energy. Am Mineral 105, 136–140. doi:10.2138/am-2020-7228

Beane R, Wiebe R (2012). Origin of quartz clusters in Vinalhaven granite and porphyry, coastal Maine. Contrib Mineral Petrol 163, 1069-1082. https://doi.org/10.1007/s00410-011-0717-1

Bennett EN, Jenner FE, Millet MA, Cashman KV, Lissenberg CJ (2019). Deep roots for mid-ocean-ridge volcanoes revealed by plagioclase-hosted melt inclusions. Nature 572, 235–239. https://doi.org/10.1038/s41586-019-1448-0

Bergantz G, Schleicher J, Burgisser A (2015). Open-system dynamics and mixing in magma mushes. Nature Geoscience 8, 793-796.

Bertolett EM, Prior DJ, Gravley DM, Hampton SJ, Kennedy BM (2019). Compacted cumulates revealed by electron backscatter diffraction analysis of plutonic lithics. Geology 47, 445-448. ttps://doi.org/10.1130/G45616.1

Blundy J, Cashman K (2001). Ascent-driven crystallisation of dacite magmas at mount St Helens, 1980–1986. Contrib Mineral Petrol 140, 631–650. https://doi.org/10.1007/s004100000219

Blundy J, Cashman K (2005). Rapid decompression-driven crystallization recorded by melt inclusions from Mount St. Helens volcano. Geology 33, 793–796. https://doi.org/10.1130/G21668.1

Blundy J (2022). Chemical Differentiation by Mineralogical Buffering in Crustal Hot Zones. J Petrol 63, egac054. https://doi.org/10.1093/petrology/egac054

Bohrson WA, Spera FJ, Ghiorso MS, Brown GA, Creamer JB, Mayfield A (2014). Thermodynamic model for energy-constrained open-system evolution of crustal magma bodies undergoing simultaneous recharge, assimilation and crystallization: the magma chamber simulator. Journal of Petrology 55, 1685–1717.

Cao M, Evans NJ, Reddy SM, Fougerouse D, Hollings P, Saxey DW, McInnes BI, Cooke DR, McDonald BJ, Qin K (2019). Micro- and nano-scale textural and compositional zonation in plagioclase at the Black Mountain porphyry Cu deposit: Implications for magmatic processes. American Mineralogist 104, 391–402.

Camejo-Harry M, Melekhova E, Blundy J, Attridge W, Robertson R, Christopher T (2018). Magma evolution beneath Bequia, Lesser Antilles, deduced from petrology of lavas and plutonic xenoliths. Contrib Mineral Petrol 173, 77. https://doi .org /10 .1007 /s00410-018-1504-z

Chamberlain KJ, Wilson CJN, Wallace PJ, Millet MA (2015). Micro-analytical perspectives on the Bishop Tuff and its magma chamber. J Petrol 56, 605–640. https://doi.org/10.1093/petrology/egv012

Cheng L, Costa F, Bergantz G (2020). Linking fluid dynamics and olivine crystal scale zoning during simulated magma intrusion. Contributions to Mineralogy and Petrology 175, 53.

Cornet J, Bachmann O, Ganne J, Fiedrich A, Huber C, Deering CD, et al. (2022). Assessing the effect of melt extraction from mushy reservoirs on compositions of granitoids; from a global database to a single batholith. Geosphere 18, 985–999. https://doi.org/10.1130/GES02333.1

Corsaro RA, Miraglia L (2022). Near Real-Time Petrologic Monitoring on Volcanic Glass to Infer Magmatic Processes During the February–April 2021 Paroxysms of the South-East Crater, Etna. Front Earth Sci 10:828026. https://doi.org/10.3389/feart.2022.828026

Crabtree SM, Lange RA (2011). Complex Phenocryst textures and zoning patterns in Andesites and Dacites: evidence of degassing-induced rapid crystallization? Journal of Petrology 52, 3–38.

Dayton K et al. (2023). Deep magma storage during the 2021 La Palma eruption. Sci Adv 9, eade7641. https://doi.org/10.1126/sciadv.ade7641/

Davidson JP, Morgan DJ, Charlier BLA, Harlou R, Hora JM (2007). Microsampling and isotopic analysis of igneous rocks; implications for the study of magmatic systems. Ann Rev Earth Planet Sci 35, 273–311. https://doi.org/10.1146/annurev.earth.35.031306.140211

Deering CD, Bachmann O (2010). Trace element indicators of crystal accumulation in silicic igneous rocks. Earth and Planetary Science Letters, 297, 324-331. https://doi.org/10.1016/j.epsl.2010.06.034

Deering CD, Bachmann O, Vogel TA (2011). The Ammonia Tanks Tuff: Erupting a melt-rich rhyolite cap and its remobilized crystal cumulate. Earth and Planetary Science Letters, 310(3-4): 518-525. https://doi.org/10.1016/j.epsl.2011.08.032

DeVitre C, Wieser P (2024). Reliability of Raman analyses of CO_2-rich fluid inclusions as a geobarometer at Kīlauea. Geochemical Perspective Letters 29. https://doi.org/10.7185/geochemlet.2404

Edmonds M, Cashman, KV, Holness, M, Jackson M (2019). Architecture and dynamics of magma reservoirs. The Royal Society Publishing 377, 20180298.

Erdmann S, Martel C, Pichavant M, Kushnir A (2014). Amphibole as an archivist of magmatic crystallization conditions: problems, potential, and implications for inferring magma storage prior to the paroxysmal 2010 eruption of Mount Merapi, Indonesia. Contrib Mineral Petrol 167, 1016. https://doi.org/10.1007/s00410-014-1016-4

Fiedrich AM et al. (2017). Mineralogical, geochemical, and textural indicators of crystal accumulation in the Adamello Batholith (Northern Italy). Am Mineral 102, 2467-2483. ttps://doi.org/10.2138/am-2017-6026

Forni F et al. (2015). Erupted cumulate fragments in rhyolites from Lipari (Aeolian Islands). Contrib Mineral Petrol 170, 1-18. https://doi.org/10.1007/s00410-015-1201-0

Gansecki C et al. (2019). The tangled tale of Kīlauea's 2018 eruption as told by geochemical monitoring. Science 366, eaaz0147. https://10.1126/science.aaz0147

Giacomoni PP, Ferlito C, Coltorti M, Bonadiman C, Lanzafame G (2014). Plagioclase as archive of magma ascent dynamics on 'open conduit' volcanoes: the2001–2006 eruptive period at Mt.Etna. Earth-Science Reviews 138, 371–393.

Glazner AF, Coleman DS, Mills RD (2015). The Volcanic-Plutonic Connection. Advances in Volcanology. Springer Berlin Heidelberg, 1-22.

Glazner AF (2021). Thermal constraints on the longevity, depth, and vertical extent of magmatic systems. Geochem Geophys Geosys 22, e2020GC009459. https://doi.org/10.1029/2020GC009459

Gleeson MLM, Gibson SA, Stock MJ (2021). Upper mantle mush zones beneath low melt flux ocean island volcanoes; insights from Isla Floreana, Galapagos. J Petrol 61, egaa094. https://doi.org/10.1093/petrology/egaa094

Graeter KA, Beane RJ, Deering CD, Gravley D, Bachmann O (2015). Formation of rhyolite at the Okataina Volcanic Complex, New Zealand: New insights from analysis of quartz clusters in plutonic lithics. Am Mineral 100, 1778-1789. https://doi.org/10.2138/am-2015-5135

Ghiorso MS, Evans BW (2008). Thermodynamics of rhombohedral oxide solid solutions and a revision of the Fe-Ti two-oxide geothermometer and oxygen-barometer. American Journal of Science 308, 957-1039. https://doi.org/10.2475/09.2008.01

Gualda GAR, Cook DL, Chopra R, Qin L, Anderson Jr AT, Rivers M (2004). Fragmentation, nucleation and migration of crystals and bubbles in the Bishop Tuff rhyolitic magma. Transactions of the Royal Society of Edinburgh: Earth Sciences 95, 375–390.

Gualda GAR, Pamukcu AS, Ghiorso MS, Anderson AT, Sutton SR, Rivers ML (2012). Timescales of quartz crystallization and the longevity of the Bishop giant magma body. PloS one, e37492–e37492. https://doi.org/10.1371/journal.pone.0037492

Gualda GAR, Gravley DM, Connor M, Hollmann B, Pamukcu AS, Bégué F, et al. (2018). Climbing the crustal ladder : magma storage-depth evolution during a volcanic flare-up. Sci Adv 4, eaap7567. https://doi.org/10.1126/sciadv.aap7567

Gualda GAR, Ghiorso MS, Hurst AA, Allen MC, Bradshaw RW (2022). A complex patchwork of magma bodies that fed the Bishop Tuff supereruption (Long Valley Caldera, CA, United States): Evidence from matrix glass major and trace-element compositions. Front Earth Sci 10, 798387. https://doi.org/10.3389/feart.2022.798387

Hanchar JM, Watson EB (2003). Zircon Saturation Thermometry. Reviews in Mineralogy and Geochemistry 53, 89–112. https://doi.org/10.2113/0530089

Hansteen TH, Klügel A (2008). Fluid Inclusion Thermobarometry as a Tracer for Magmatic Processes. Rev Mineral Geochem 69, 143–178. https://doi.org/10.2138/rmg.2008.69.5

Higgins O, Sheldrake T, Caricchi L (2022). Machine learning thermobarometry and chemometry using amphibole and clinopyroxene: a window into the roots of an arc volcano (mount Liamuiga, saint Kitts). Contrib Mineral Petrol 177, 10. https://doi.org/10.1007/s00410-021-01874-6

Higgins O, Stock MJ (2024). A new calibration of the OPAM thermobarometer for anhydrous and hydrous mafic systems. J Petrol 65. https://doi.org/10.1093/petrology/egae043

Hildreth W, Moorbath S (1988). Crustal contributions to arc magmatism in the Andes of Central Chile. Contr Mineral Petrol 98, 455–489. https://doi.org/10.1007/BF00372365

Hildreth W, Wilson CJN (2007). Compositional Zoning of the Bishop Tuff. J Petrol 48, 951–999. https://doi.org/10.1093/petrology/egm007

Holland TJB, Green ECR, Powell R (2018). Melting of Peridotites through to Granites: A Simple Thermodynamic Model in the System KNCFMASHTOCr. Journal of Petrology 59, 881–900. https://doi.org/10.1093/PETROLOGY/EGY048

Iacovino K et al (2021). VESIcal Part I: An Open-Source Thermodynamic Model Engine for Mixed Volatile (H_2O-CO_2) Solubility in Silicate Melts. Earth Space Sci https://doi.org/10.1029/2020EA001584

Jackson MD, Blundy J, Sparks RSJ (2018). Chemical differentiation, cold storage and remobilization of magma in the Earth's crust. Nature 564, 405–409. https://doi.org/10.1038/s41586-018-0746-2

Jorgenson C, Higgins O, Petrelli M, Bégué F, Caricchi L (2022). A machine learning based approach to clinopyroxene thermobarometry: Model optimisation and distribution for use in earth sciences. Journal of Geophysical Research: Solid Earth, e2021JB022904. https://doi.org/10.1029/2021JB022904

Kent AJR (2008). Melt Inclusions in Basaltic and Related Volcanic Rocks. Rev Mineral Geochem 69, 273–331. https://doi.org/10.2138/rmg.2008.69.8

Kent AJ, Till CB, Cooper KM (2023). Start me up: The relationship between volcanic eruption characteristics and eruption initiation mechanisms. Volcanica 6, 161-172.

Lee CTA, Morton DM (2015). High silica granites: Terminal porosity and crystal settling in shallow magma chambers. Earth Planet Sci Lett 409, 23-31. https://doi.org/10.1016/j.epsl.2014.10.040

Li X, Zhang C (2022). Machine learning thermobarometry for biotite-bearing magmas. J Geophys Res: Solid Earth 127, e2022JB024137. https://doi.org/10.1029/2022JB024137Citations: 8

MacDonald A, Ubide T, Mollo S, Pontesilli A, Masotta M (2023). The influence of undercooling and sector zoning on clinopyroxene–melt equilibrium and thermobarometry. J Petrol 64, 1–18, https://doi.org/10.1093/petrology/egad074

Maclennan J, McKenzie D, Hilton F, Gronvöld K, Shimizu N (2003). Geochemical variability in a single flow from northern Iceland. Journal of Geophysical Research: Solid Earth 108(B1), ECV-4. https://doi.org/10.1029/2000JB000142

Maclennan J (2017). Bubble formation and decrepitation control the CO_2 content of olivine-hosted melt inclusions. Geochem Geophys Geosyst 18, 597–616. https://doi.org/10.1002/2016GC006633

Marsh BD (2004). A magmatic mush column rosetta stone: The McMurdo Dry Valleys of Antarctica. EOS, Transactions of the American Geophysical Union 85(47): 497 and 502. https://doi.org/10.1029/2004EO470001

Masotta M et al. (2020). The role of undercooling during clinopyroxene growth in trachybasaltic magmas: Insights on magma decompression and cooling at Mt. Etna volcano. Geochimica et Cosmochimica Acta 268, 258–276.

Médard E, Le Pennec JL (2022). Petrologic imaging of the magma reservoirs that feed large silicic eruptions. Lithos 428–429, 106812. https://doi.org/10.1016/j.lithos.2022.106812

Moore LR, Gazel E, Tuohy R, Lloyd AS, Esposito R, Steele-MacInnis M, Hauri EH, Wallace PJ, Plank T, Bodnar RJ (2015). Bubbles matter: An assessment of the contribution of vapor bubbles to melt inclusion volatile budgets. American Mineralogist 100(4), 806-823. https://doi.org/10.2138/am-2015-5036

Mourey AJ, Shea T (2019). Forming Olivine Phenocrysts in Basalt: A 3D Characterization of Growth Rates in Laboratory Experiments. Front Earth Sci 7, 300. https://doi.org/10.3389/feart.2019.00300

Mulder J, Hagen-Peter G, Ubide T, Andreasen R, Kooijman E, Kielman-Schmitt M, et al. (2023). New Reference Materials, Analytical Procedures and Data Reduction Strategies for Sr Isotope Measurements in Geological Materials by LA-MC-ICP-MS. Geostand Geoanal Res 47, 311–36. https://doi.org/10.1111/ggr.12480

Mutch EJF, Blundy JD, Tattitch BC, Cooper FJ, Brooker RA (2016). An experimental study of amphibole stability in low-pressure granitic magmas and a revised Al-in-hornblende geobarometer. Contributions to Mineralogy and Petrology 171, 1-27

Mutch EJF, Maclennan J, Shorttle O, Edmonds M, Rudge JF (2019). Rapid transcrustal magma movement under Iceland. Nature Geoscience 12, 569-574.

Neave DA, Passmore E, Maclennan J, Fitton G, Thordarson T (2013). Crystal–melt relationships and the record of deep mixing and crystallization in the ad 1783 Laki Eruption, Iceland. J Petrol 54, 1661–1690. https://doi.org/10.1093/petrology/egt027

Neave DA, Putirka KD (2017). A new clinopyroxene-liquid barometer, and implications for magma storage pressures under Icelandic rift zones. Am Mineral 102, 777–794. https://doi.org/10.2138/am-2017-5968

Neave DA, Bali E, Guðfinnsson GH, Halldórsson SA, Kahl M, Schmidt AS, Holtz F (2019). Clinopyroxene–liquid equilibria and geothermobarometry in natural and experimental tholeiites: the 2014–2015 Holuhraun eruption, Iceland. J Petrol 60, 1653–1680. https://doi.org/10.1093/petrology/egz042

Otamendi JE et al. (2020). The geodynamic history of the Famatinian arc, Argentina: A record of exposed geology over the type section (latitudes 27°- 33° south). Journal of South American Earth Sciences 100, 102558. https://doi.org/10.1016/j.jsames.2020.102558

Pallister JS, Hoblitt RP, Reyes AG (1992). A basalt trigger for the 1991 eruptions of Pinatubo volcano? Nature 356, 426–428. https://doi.org/10.1038/356426a0

Pamukcu AS, Gualda GAR, Anderson AT (2012). Crystallization stages of the Bishop Tuff magma body recorded in crystal textures in pumice clasts. J Petrol 53, 589–609. https://doi.org/10.1093/petrology/egr072

Pamukcu AS, Gualda GAR, Begue F, Gravley DM (2015). Melt inclusion shapes; timekeepers of short-lived giant magma bodies. Geology 43, 947–50. https://doi.org/10.1130/G37021.1

Pankhurst MJ, Scarrow JH, Barbee OA, Hickey J, Coldwell BC, Rollinson GK, et al. (2022). Rapid response petrology for the opening eruptive phase of the 2021 Cumbre Vieja eruption, La Palma, Canary Islands. Volcanica 5, 1–10. https://doi.org/10.30909/vol.05.01.0110

Putirka K (2016). Amphibole thermometers and barometers for igneous systems and some implications for eruption mechanisms of felsic magmas at arc volcanoes. Am Mineral 101, 841–58. https://doi.org/10.2138/am-2016-5506

Rasmussen DJ, Plank TA, Roman DC, Zimmer MM (2022). Magmatic water content controls the pre-eruptive depth of arc magmas. Science 375, 1169-1172. https://doi.org/10.1126/science.abm5174

Riel N, Kaus BJ, Green ECR, Berlie N (2022). MAGEMin, an efficient Gibbs energy minimizer: application to igneous systems. Geochemistry, Geophysics, Geosystems 23(7), p.e2022GC010427. https://doi.org/10.1029/2022GC010427

Schaen AJ et al (2017). Complementary crystal accumulation and rhyolite melt segregation in a late Miocene Andean pluton. Geology 45, 835-838. https://doi.org/10.1130/G39167.1

Špillar V, Dolejš D (2015). Melt extraction from crystal mushes: Numerical model of texture evolution and calibration of crystallinity-ordering relationships. Lithos 239, 19-32. https://doi.org/10.1016/j.lithos.2015.10.001

Stock M, Humphreys M, Smith V et al. (2016). Late-stage volatile saturation as a potential trigger for explosive volcanic eruptions. Nature Geosci 9, 249–254. https://doi.org/10.1038/ngeo2639

Stock MJ et al. (2020). Cryptic evolved melts beneath monotonous basaltic shield volcanoes in the Galápagos Archipelago. Nat Commun 11, 3767.

Streck MJ, Putirka KD, Tepley FJ (2008). Mineral textures and zoning as evidence for open system processes. Reviews in Mineralogy and Geochemistry 69, 595–622. https://doi.org/10.2138/rmg.2008.69.15

Tapu AT, Ubide T, Vasconcelos PM (2023). Increasing complexity in magmatic architecture of volcanoes along a waning hotspot. Nat Geosci 16, 371–379. https://doi.org/10.1038/s41561-023-01156-9

Tsuchiyama A (1985). Dissolution kinetics of plagioclase in the melt of the system diopside-albite-anorthite, and origin of dusty plagioclase in andesites. Contributions to Mineralogy and Petrology 89, 1–16.

Ubide T, Caulfield J, Brandt C, Bussweiler Y, Mollo S, Di Stefano F, Nazzari M, Scarlato P (2024). Deep magma storage revealed by multi-method elemental mapping of clinopyroxene megacrysts at Stromboli volcano. Frontiers in earth science. 2019, 7. https://doi.org/10.3389/feart.2019.00239

Ubide T, Larrea P, Becerril L, Gale C (2022). Volcanic plumbing filters on ocean-island basalt geochemistry. Geology 50, 26–31. https://doi.org/10.1130/G49224.1

Ubide T, Márquez Álvaro, Ancochea E, Huertas MJ, Herrera R, Coello-Bravo JJ, et al. (2023). Discrete magma injections drive the 2021 La Palma eruption. Sci Adv 9, eadg4813. https://doi.org/10.1126/sciadv.adg4813

Vlastelic I, Sainlot N, Samaniego P, Bernard B, Nauret F, Hidalgo S, et al. (2023). Arc volcano activity driven by small-scale metasomatism of the magma source. Nature Geosci 16, 363–70. https://doi.org/10.1038/s41561-023-01143-0

Wallace PJ, Anderson AT, Davis AM (1999). Gradients in H_2O, CO_2, and exsolved gas in a large-volume silicic magma system: Interpreting the record preserved in melt inclusions from the Bishop Tuff. J Geophys Res 104, 20097–20122. https://doi.org/10.1029/1999jb900207

Wark DA, Hildreth W, Spear FS, Cherniak DJ, Watson EB (2007). Pre-eruption recharge of the Bishop magma system. Geology 35, 235–238. https://doi.org/10.1130/G23316a.1

Weber G, Blundy J (2024). A machine learning-based thermobarometer for magmatic liquids. J Petrol 65, egae020. https://doi.org/10.1093/petrology/egae020

Weller OM, Holland TJB, Soderman CR, Green ECR, Powell R, Beard CD, Riel N (2024). New thermodynamic models for anhydrous alkaline-silicate magmatic systems. Journal of Petrology, egae098, https://doi.org/10.1093/petrology/egae098

Wieser PE, Kent AJ, Till CB (2023). Barometers behaving badly II: A critical evaluation of Cpx-only and Cpx-Liq thermobarometry in variably-hydrous arc magmas. Journal of Petrology 64(8), p.egad050.

Wieser PE, Kent AJ, Till CB, Donovan J, Neave DA, Blatter DL, Krawczynski MJ (2023). Barometers behaving badly I: Assessing the influence of analytical and experimental uncertainty on clinopyroxene thermobarometry calculations at crustal conditions. Journal of Petrology 64(2), p.egac126.

Wolff JA et al. (2015). Remelting of cumulates as a process for producing chemical zoning in silicic tuffs: A comparison of cool, wet and hot, dry rhyolitic magma systems. Lithos 236-237, 275-286. https://doi.org/10.1016/j.lithos.2015.09.002

Wolff JA (2017). On the syenite-trachyte problem. Geology 45, 1067-1070. https://doi.org/10.1130/G39415.1

Zanon V, D'Auria L, Schiavi F, Cyrzan K, Pankhurst MJ (2024). Toward a near real-time magma ascent monitoring by combined fluid inclusion barometry and ongoing seismicity. Sci Adv 10, eadi4300. http://doi.org/10.1126/sciadv.adi4300

Zellmer GF (2021). Gaining acuity on crystal terminology in volcanic rocks. Bull Volcanol 83, 78. https://doi.org/10.1007/s00445-021-01505-9

Zellmer GF, Iizuka Y, Straub SM (2024). Origin of crystals in mafic to intermediate magmas from Circum-Pacific continental arcs: transcrustal magmatic systems versus transcrustal plutonic systems. J Petrol 65, egae013. https://doi.org/10.1093/petrology/egae013

Figure 1 - PETROLOGICAL CHARACTERISATION OF MAGMA STORAGE

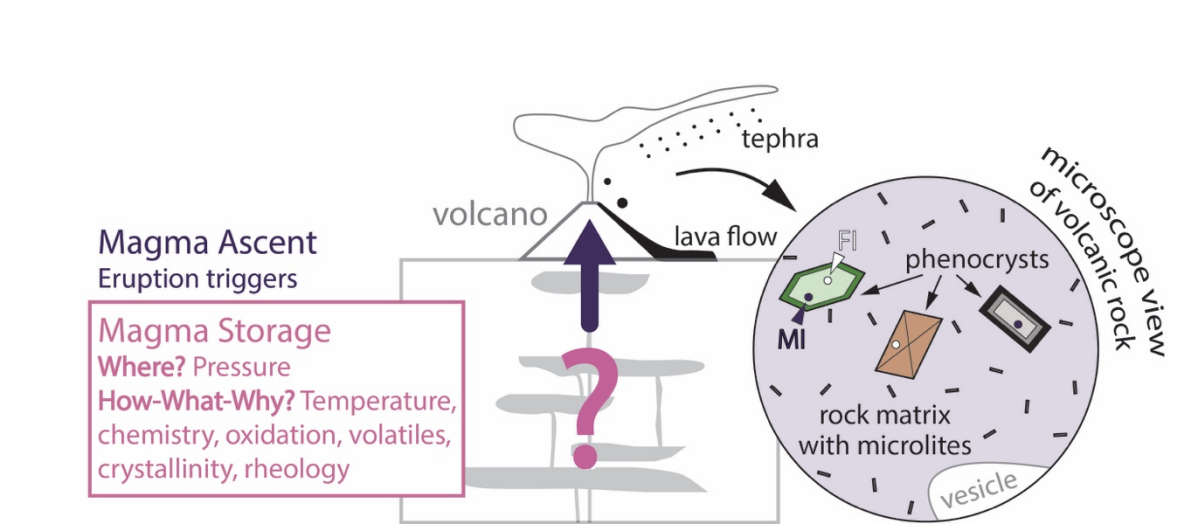

Figure 1. Active volcano plumbing systems are inaccessible to direct observation but can be reconstructed from the mineral, melt, and volatile information contained in volcanic rocks. The depth and characteristics of storage, and the conditions that lead to stalling vs eruption, can be determined using information locked in erupted rocks (and fossilised plutons). Sketched phenocrysts represent minerals typical in mafic magmas: olivine with concentric zoning, clinopyroxene with sector zoning, and plagioclase with oscillatory zoning from left to right; the same approach applies to intermediate to felsic magma compositions with more evolved mineral assemblages. FI: fluid inclusion. MI: melt inclusion. Plutonic fragments and crystal-rich clasts (not sketched) provide additional information on magma feeder systems. Petrological constraints on storage conditions can then be interpreted in the context of regional rheological boundaries (mantle-crust, lithological changes in crustal column) and combined with geophysical information (chapter 1.4.1) and timescales of magmatic processes (chapter 1.4.3).

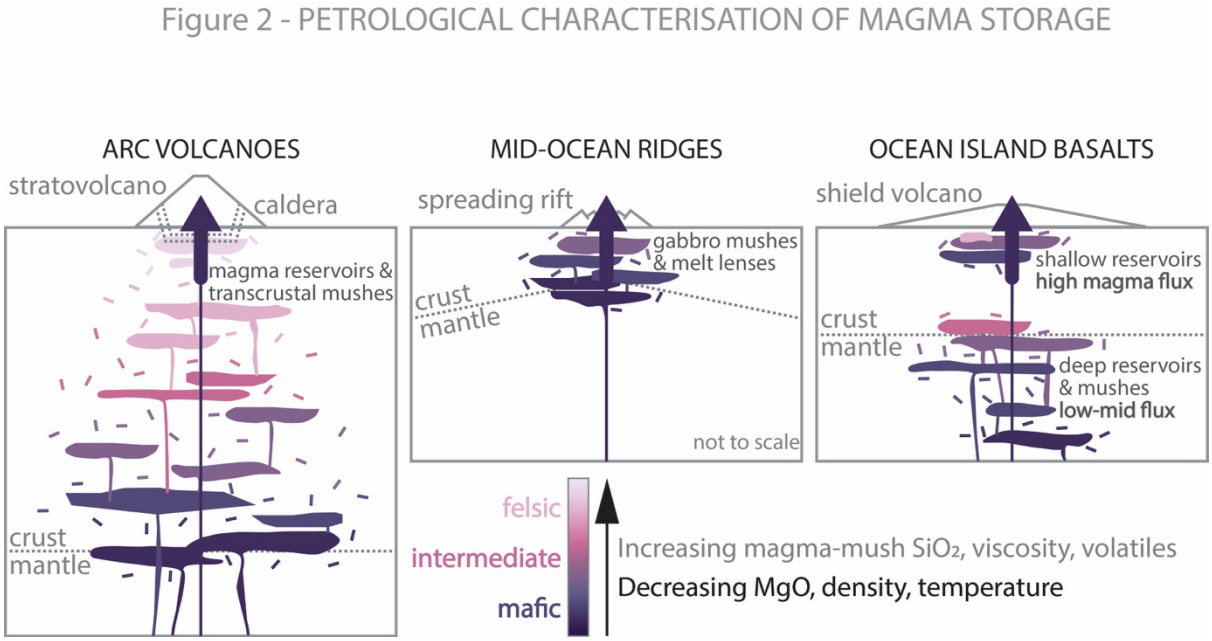

Figure 2. Conceptual models for magma-mush storage systems across tectonic settings. Growing evidence from geophysical (chapter 1.4.1) and petrological (this chapter) work suggests magma plumbing systems are commonly dominated by crystal mushes with ephemeral eruptible melt pockets (exaggerated for sketching purposes). Colours represent magma-mush composition (more evolved with increasing SiO_2), and typical volcano morphologies are added to each tectonic setting, noting they are not exclusive to the depicted settings. Left: Continuous transcrustal storage [1] requires strong heat flux and may develop at the peak of magmatism in arc systems. More typically, storage may be less continuous even if multi-level. The thick crust in continental arcs promotes prolonged magma storage and evolution relative to oceanic arcs and other settings. Shallow storage enhances cooling and differentiation and may lead to explosive volcanism, including caldera-forming eruptions. Middle: In mid-ocean ridges, the limited magmatic journey from shallow magma generation to eruption limits differentiation, with ocean spreading rates controlling magma supply and melt fraction in the mush [2]. Right: In oceanic islands, depth of storage correlates with eruption frequency, considered a proxy for magma flux. Systems with low magma flux like the Canary Islands or Cape Verde are primarily fed directly by upper mantle reservoirs with limited crustal storage [3], whereas high magma flux systems like Hawaii or Réunion develop a stable reservoir at shallow depth [4].

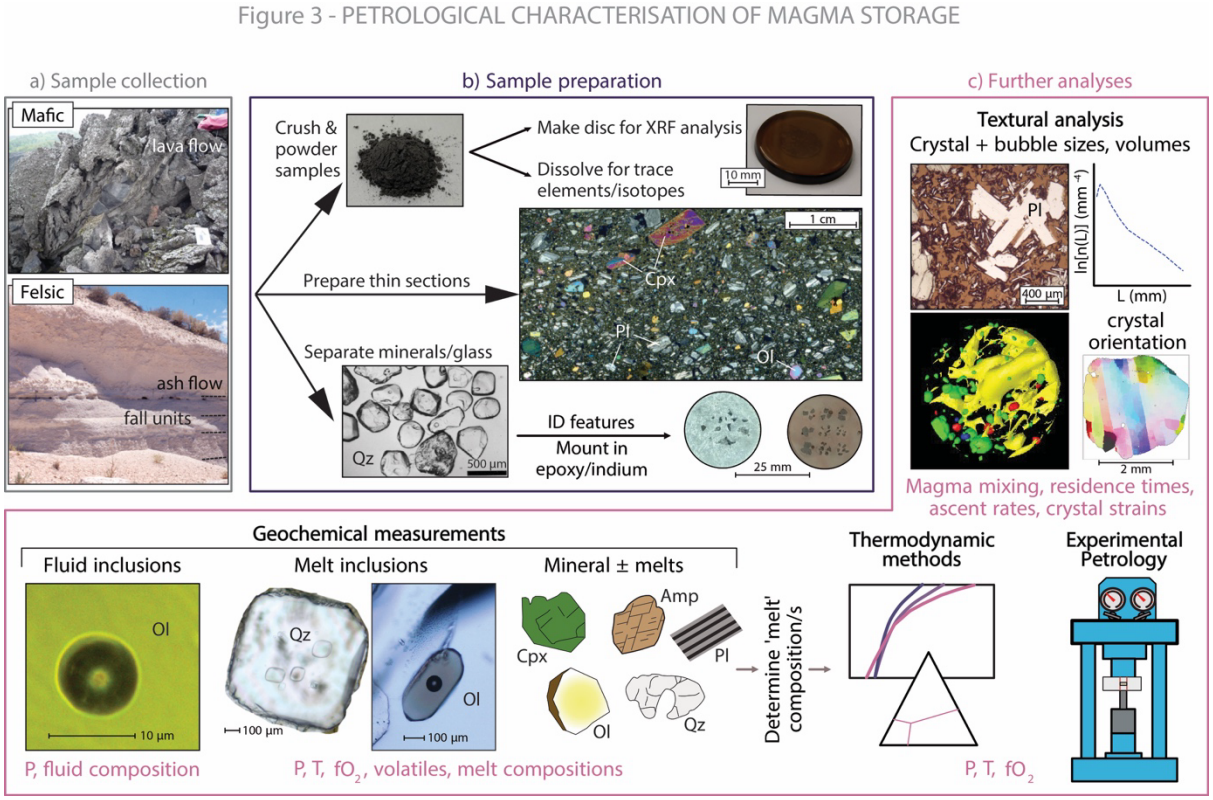

Figure 3. Example workflow to investigate magma storage conditions using petrology. After sample collection (a), a wide variety of sample preparation strategies may be used (b), such as powdering for bulk analysis, making thin sections to examine textures and perform analysis of minerals, matrix or glass, and/or separate out individual crystals and features for highly targeted analyses. c) Then, a variety of geochemical and textural measurements can be used to determine the conditions and processes occurring in magma reservoirs prior to eruption (pink text). Basic chemical measurements of rock, matrix, glass and mineral compositions are also used to perform thermodynamic calculations and experiments to try to recreate the minerals and textures seen in the natural samples (cf. How-to Box). Mineral examples include Ol-olivine, Qz-quartz, Cpx-clinopyroxene, Amp-amphibole, Pl-plagioclase. Quartz-hosted melt inclusion picture kindly supplied by Madison Myers, and pictures of rock powder and XRF disc kindly supplied by John Caulfield.

Figure 4 - PETROLOGICAL CHARACTERISATION OF MAGMA STORAGE

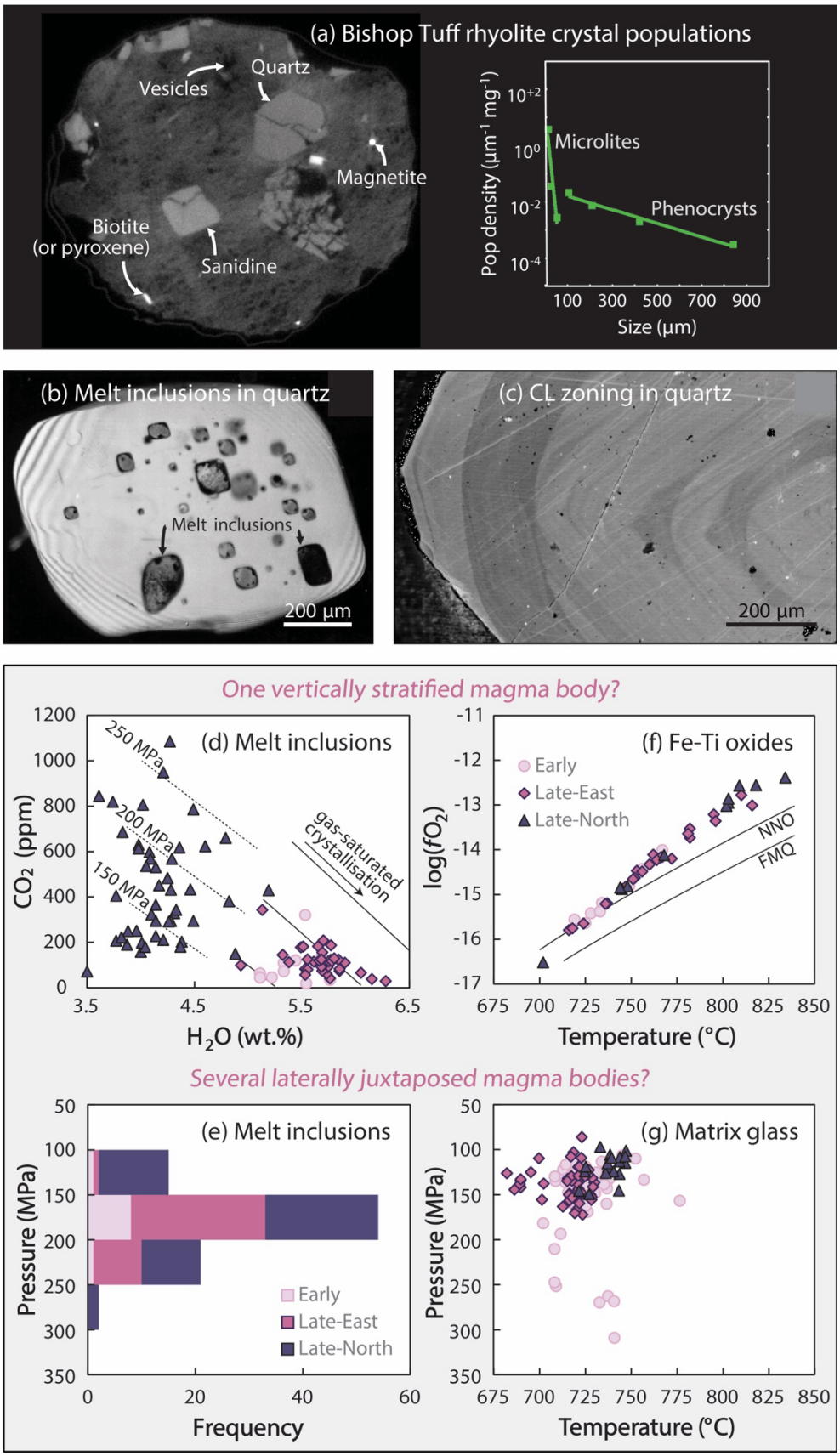

Figure 4. Example of conflicting evidence on magma storage from the 765 ka Bishop Tuff, Long Valley Caldera, California (Case study Box 2) from a variety of data sources (cf. further reading website list and [21]). The records of Fe-Ti oxides and H_2O-CO_2 saturation pressures have been interpreted as suggestive of a vertically stratified magma body, with some of the magmas being fluid-undersaturated. In contrast, zircon-saturation temperatures, rhyolite-MELTS quartz-2feldspar-saturation pressures and H_2O-CO_2 pressures have been interpreted as consistent with laterally juxtaposed, fluid saturated magma bodies. The differences in interpretation highlight the non-unique ways in which data can be explained, and the need for additional data and lines of evidence to resolve inconsistencies. (a) X-ray computed tomography data from Bishop Tuff pumice. Left image shows a slice through the reconstructed volume (grey intensity correlated with mean atomic number, similar to back-scattered electron images), with various phases identified. On the right, crystal size distribution diagram of population density vs. crystal size shows two distinct populations: large crystals (phenocrysts) are interpreted to represent pre-eruptive growth, while small crystals (microlites) are interpreted to represent syn-eruptive nucleation and growth. (b) Quartz crystal immersed in refractive index oil, showing numerous melt inclusions (two examples indicated). (c) Cathodoluminescence (CL) image of quartz crystal showing bright rim; these rims have been variously interpreted as representing magma replenishment or fast crystal growth. (d,e) H_2O, CO_2, and saturation pressures determined from melt inclusions (solid and dashed isobars estimated at 725 °C and 790 °C, respectively). The same data are interpreted differently by different authors – the original authors suggested the Late-North magmas are fluid-undersaturated (d) and later authors re-interpreted the data suggesting all magmas are fluid-saturated (e). (f) Temperature and oxygen fugacity estimates based on Fe-Ti oxides (magnetite-ilmenite). (g) Zircon-saturation temperatures and rhyolite-MELTS quartz-2feldspar-saturation pressures from matrix glass compositions.

Figure 5 - PETROLOGICAL CHARACTERISATION OF MAGMA STORAGE

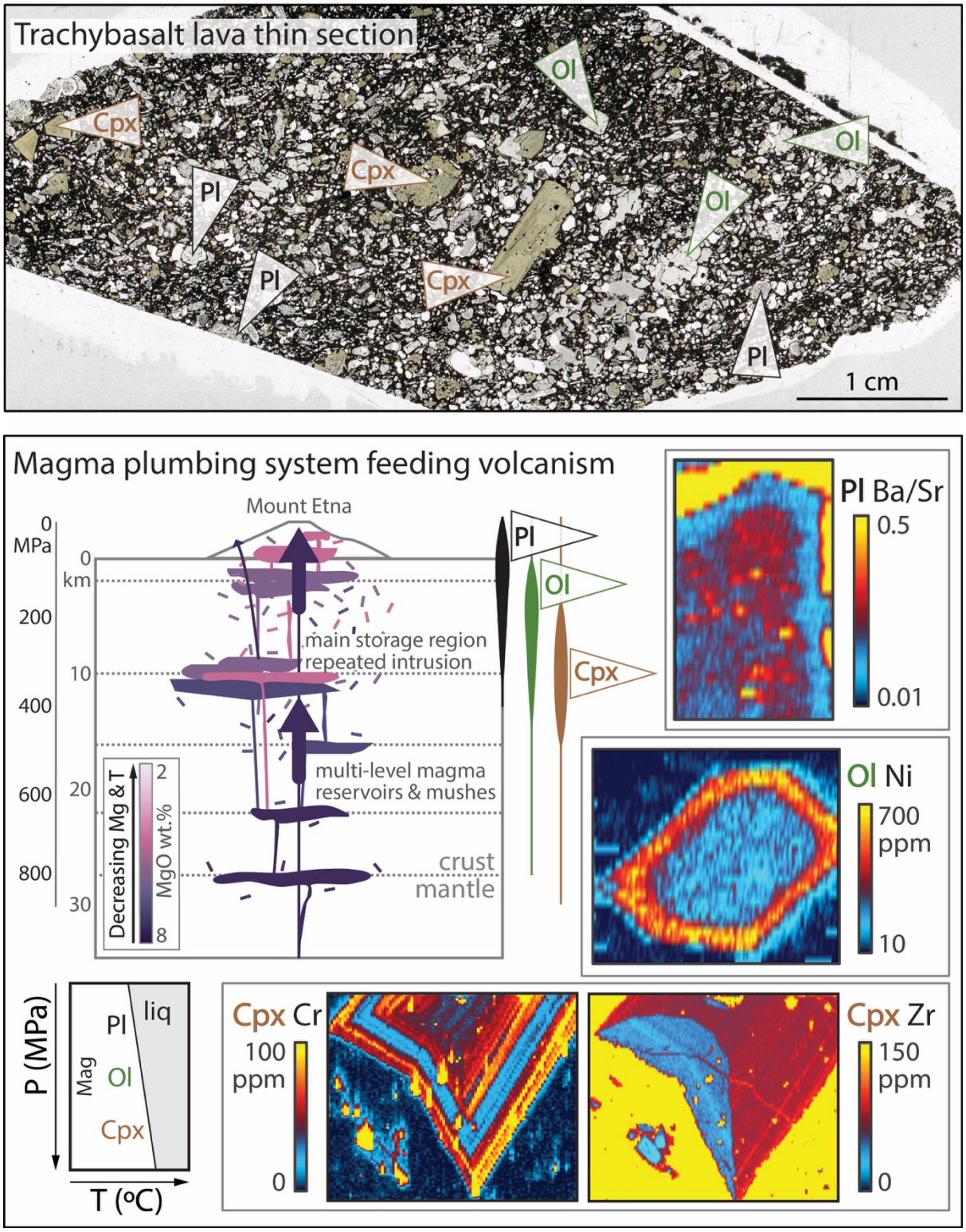

Figure 5. Phenocrysts in erupted rocks may record different parts and processes of the ascent history through the plumbing system, as exemplified at Mount Etna (Sicily, Italy), one of the most active and best monitored volcanoes on Earth. Top: trachybasalt thin section

with phenocrysts of clinopyroxene (Cpx), olivine (Ol) and plagioclase (Pl) recycled by ascending magmas from the feeder system. Bottom: sketch of the magma plumbing system, highlighting storage along crustal discontinuities (grey dashed lines) and particularly along the carbonate-granitoid boundary at ~10 km depth and shallower depths linked to degassing-induced crystallisation (modified from [7]); colours of reservoirs and mush broadly follow the colour scale in Fig. 2; lighter colours represent decreasing magmatic temperature with decreasing magnesium content in Mount Etna magmas. The simplified phase diagram at the bottom left corner highlights the effect of pressure on the liquidus assemblage, with clinopyroxene stability expanded at depth (Mag: titanomagnetite). On the right, elemental maps obtained by LA-ICP-MS visualise zoning patterns that differ across the phenocryst assemblage (ppm parts per million). All minerals show distinct rims suggesting mafic recharge prior to eruption, i.e., high Cr and low Zr concentrations in clinopyroxene, high Ni concentrations in olivine, low Ba/Sr ratios in plagioclase. However, their core records differ. Clinopyroxene shows oscillatory and sector zoning archiving repeated magma replenishment and mixing (note variations in Cr primarily respond to oscillatory zoning whilst variations in Zr in the same crystal are primarily controlled by sector zoning; [11]). The apparently simpler record in olivine may be partly due to faster chemical diffusion, leading to obliteration of zoning patterns during magma storage but allowing modelling of timescales of recharge to eruption (chapter 1.4.3). Plagioclase stability expands at low pressure and particularly with the loss of magmatic water (degassing), recording shallower processes relative to clinopyroxene.

How-to Box: Petrological tools to estimate where and how magmas are stored before eruption

Mineral ± melt thermobarometry - Reactions between chemical components in liquid and mineral phases (e.g., clinopyroxene-liquid or clinopyroxene-orthopyroxene) and mineral compositions (e.g., amphiboles) are sensitive to pressure and temperature. Barometers (sensitive to pressure) rely on reactions with a large change in volume, while thermometers rely on reactions with a large change in entropy. In reality, most reactions are sensitive to both pressure and temperature, so barometers and thermometers are often iteratively solved, noting that *P* and *T* in the experiments used for calibration are not always independent parameters and this may introduce bias in the calculations. Thermobarometers are calibrated using a dataset of experiments where pressure and temperature are known, and various regression strategies are used to relate mineral and melt composition to *P* and *T*. Empirical regressions may have terms routed in thermodynamics, with the addition of empirical terms to improve fit. Alternatively, recent algorithms use machine learning techniques (e.g., random forests), where the model is trained on the relationship between measured oxide contents and intensive variables without knowledge of the thermodynamics of the system.

Melt inclusion barometry - Melt inclusions are pockets of melt that become trapped within growing crystals, effectively isolating a record of the melt composition at depth in the volcanic system. The amounts of H_2O and CO_2 that dissolve in a magma are strongly sensitive to pressure, in addition to temperature and melt composition. This relationship is described using a solubility law calibrated using experiments done at a wide range of pressures, temperatures, and volatile contents. By measuring volatile species in melt inclusions trapped from a volatile-saturated magma, pressures can be calculated using a solubility model. If a magma is volatile undersaturated at the time of entrapment, melt inclusion barometry will yield minimum entrapment depths. Melt inclusions are also subject to various processes which occur after their entrapment (e.g., diffusive H^+ exchange with the degassing melt outside the crystal, leakage of the inclusion by decrepitation, crystallization of the host mineral on the walls of the inclusion) which may result in pressures being underestimated.

Fluid inclusion barometry - As crystals grow, they also trap pockets of fluid (fluid inclusions). In CO_2-rich systems, the density of the trapped fluid is strongly sensitive to the pressure at which the inclusion was trapped, and relatively insensitive to temperature. CO_2 densities can be measured by microthermometry or Raman spectroscopy, and then pressures are calculated using an equation of state for an estimated entrapment temperature. Fluid inclusions are sensitive to re-equilibration - if magma stalls at shallower levels, the trapped fluid inclusion will have higher pressure than the outside melt, so the inclusion will increase its volume by plastic deformation, decreasing the CO_2 density. This means fluid inclusions may record the depth of main storage zone and depth if magmas ascended quickly with minimal stalling, and/or the depth of temporary storage zones during ascent, depending on the timescales of stalling relative to re-equilibration timescales, which are themselves very sensitive to pressure differences, temperature, and the size of the fluid inclusion.

Melt (Liquid) thermobarometry - Silicate melts (or liquids) saturated in multiple phases have a low degree of thermodynamic freedom (limited variation of intensive parameters), so the melt composition provides insights into the *P*-*T*-f_{O2} conditions of magma storage. These relationships can be calibrated empirically using experiments, or unknowns can be solved using thermodynamic models such as MELTS. Common multi-phase assemblages used for thermobarometry include olivine-plagioclase-augite (OPAM), quartz-two feldspars and plagioclase-two pyroxenes, as well as new machine learning models that consider melt saturation with multi-phase assemblages from the main mineral groups (olivine, orthopyroxene, clinopyroxene, amphibole, biotite, plagioclase, K-feldspar, quartz, garnet, magnetite and/or ilmenite).

Experimental petrology - Experiments subject a specified magma composition to known *P*, *T*, H_2O and f_{O2} conditions, to determine the presence and composition of equilibrium phases. These experiments underpin all the methods discussed here, as they are essential to calibrate mineral thermobarometers, solubility models, and thermodynamic models of magmas. In addition, experiments can be used to determine magma storage conditions at specific volcanoes, by selecting an appropriate bulk composition, and exploring which *P*-*T*-f_{O2} conditions reproduce the phases observed in erupted lavas

Thermodynamic modelling - Thermodynamic models predict the equilibrium state of the system (e.g., phases present, composition of each phase) for specified conditions through the minimisation of energies such as the Gibbs or Helmholtz energy. In practice, two main families of thermodynamic models are used in magmatic systems: the MELTS set of models developed by Mark Ghiorso and collaborators (e.g., pMELTS, rhyolite-MELTS, alpha-MELTS, Magma Chamber Simulator), and the models developed by Roger Powell, Tim Holland and collaborators (e.g., THERMOCALC, Theriak-Domino, MAGEMin, Perple_X). The fundamental minimisation algorithm in each model can be used for a variety of calculation types such as constructing phase diagrams for a given magma composition and pressure-temperature range, or calculating changes in melt and mineral chemistry during equilibrium and fractional crystallisation.

Case study Boxes

1. **Iceland and Kīlauea: high flux basaltic systems with distinct plumbing system architectures and magma processing**

Iceland has played a central role in shaping our understanding of magma reservoir processes because of the abundance of pristine samples created by the intersection of the Mid Atlantic Ridge and the Iceland Plume in a high latitude region with little soil cover. Bulk rock and melt inclusion samples have provided vital insights into how erupted magmas are assembled from initially diverse mantle melts, resulting in geochemical heterogeneity that ranges in scale from the entire island to the products of individual eruptions like that of Fagradalsfjall in 2021. Moreover, measuring large numbers of melt inclusions from individual eruptions has demonstrated how concurrent mixing and crystallisation can erase mantle-derived geochemical variability during magma ascent, sometimes resulting in large volumes of homogenous magma like that erupted at Laki in 1783–1784 and Holuhraun in 2014–2015. The textures and compositions of crystal cargoes nonetheless preserve records of complex magmatic evolution involving the formation and disaggregation of geochemically variable crystal mushes hosting intrusions of basaltic magma. Mineral, liquid, and volatile saturation barometers indicate that Icelandic basalts are stored at a range of depths throughout the crust and the crust-mantle boundary before eruption, as envisaged by stacked sill models of crustal accretion, and transported to the surface through varied ascent paths.

Like Iceland, the magmatic plumbing system of Kīlauea Volcano, Hawaii, has been subject to extensive petrological study as a result of its near continuous eruptive activity over the last ~40 yrs. Kīlauea shows remarkably coherent temporal trends in bulk trace element and isotope geochemistry, indicating that erupted melts are mixed and homogenised in a relatively small volume storage region that is shared between many eruptions. This differs from the variations in storage pressure and chemistry between Icelandic eruptions that are indicative of storage of heterogeneous mantle melts in a number of discrete sills in the mid to lower crust. Kīlauea eruptions also show very similar major element trajectories to one another, indicating that magmas are being stored and fractionated at very similar P-H_2O-f_{O2} conditions. Geophysical imaging combined with melt and fluid inclusion barometry are indicative of magma storage in two shallow, connected reservoirs (~1-2 km and 3-5 km), which have persisted for centuries. The significantly shallower depth of storage at Kīlauea also means that most eruptions (>6 wt% MgO) only contain olivine (+chrome spinel) as a phenocryst phase, vs. the olivine-clinopyroxene-plagioclase assemblage seen in Iceland. This restricts available barometry methods to those relying on volatile species (melt and fluid inclusions), because the chemistry of olivine is not sensitive to pressure, and liquids saturated in fewer phases have too many degrees of thermodynamic freedom to be good barometers.

2. **Mount St Helens and Bishop Tuff: intermediate to evolved systems where magma storage preconditions large explosive eruptions**

Since the landmark Plinian eruption of Mount St Helens in May 1980, this volcano, located in the Cascade Range (Washington, USA), has figured prominently in the development of ideas and techniques for understanding magma storage, particularly beneath arc volcanoes. The continuation of the 1980 eruption until 1986, together with further eruption between 2004-2008, provided considerable petrological data for understanding arc volcanic systems. Complementary insight came from large geophysical datasets produced via eruption monitoring as well as by major geophysical surveys. Throughout the 1980 and 2004

eruptions, Mount St Helens produced crystal-rich dacite, containing abundant plagioclase, pyroxene, oxides and amphibole; magmas that are typical for many arc volcanoes. Dating of zircons shows that the storage system may have operated for up to 10^4-10^5 years. Erupted magmas formed through a combination of differentiation of mantle wedge-derived magmas and melting and assimilation of lower crust amphibolite, followed by complex and variable histories during residence at a range of shallow and mid crustal pressures, as recorded in the textural and compositional zoning of the crystal cargo, including plagioclase and orthopyroxene. Eruptions involved magma assembly from small magma batches in such mid-upper crustal magma reservoirs. The timing deduced from Fe-Mg diffusion in orthopyroxene correlates with the observed timing of seismic events in the magma plumbing system, suggesting these represent intrusion of new magma batches into the shallow storage system. Overall, Mount St Helens exemplifies a silicic system in which eruption is favoured over storage, with frequent eruptions of magmas of variable composition and complex crystal cargoes.

In contrast, the 765 ka Bishop Tuff rhyolitic ignimbrite (Long Valley Caldera, California, USA) represents a silicic system in which storage and homogenisation are favoured over frequent eruptions, generating very large volume, multiply saturated magmas that have comparably simpler crystal cargoes, and which are highly eruptible and lead to ultra-Plinian eruptions. Isotopic studies show that Bishop Tuff magmas are independent from preceding and succeeding magmas erupted in Long Valley, and they represent the upper crustal manifestation of the climactic phase of a large silicic system. Pioneering studies in the 1970s highlighted the zoned character of the pyroclastic deposit, with early, pyroxene-free fall and flow deposits and late, pyroxene-bearing flow deposits. Lithic contents indicated different magma types erupted from different vent areas. Detailed stratigraphic studies suggested a chronology of the eruption that lasted on the order of days to weeks, indicative of a geologically instantaneous event fed by large volumes (hundreds of km^3) of predominantly crystal-poor magma stored in the Earth's shallow crust. Zircon geochronology indicated the lifetime of the Long Valley magmatic system was in the order of tens to hundreds of thousands of years, while the crystal-poor magmas that fed the Bishop Tuff eruption formed on shorter timescales of potentially a few millennia. As shown in Fig. 4, temperatures derived from Fe-Ti oxides suggest a strong thermal gradient between early and late-erupted magmas. This is in contrast with the more limited database of zircon-saturation temperatures using glass compositions, which show only a modest difference in temperature between magmas erupted from different vents. The abundance of H_2O and CO_2 in melt inclusions was investigated in groundbreaking studies in the 1990s, returning high-H_2O and low-CO_2 for magmas erupted to the south and east (Early and Late-East in Fig. 4), and lower H_2O and higher CO_2 magmas erupted to the north (Late-North in Fig. 4). Saturation pressures for both groups are similar, but magmas erupted to the north may have been fluid-undersaturated at the time of eruption, making it possible for magmas erupted to the north to have been stored at higher pressures than magmas erupted to the south and east. This suggests the eruption was fed by a vertically stratified magma body. In contrast, pre-eruptive pressures based on quartz-2feldspar-saturation from glass compositions indicate similar pressure ranges for all magmas, suggestive of lateral juxtaposition of at least three chemically independent, fluid-saturated magma bodies. The Bishop Tuff has continuously challenged our understanding of the architecture of and processes operating in silicic magmatic systems, but it has also repeatedly opened new doors and forced us to revise our perspectives on silicic magma storage and evolution in the Earth's shallow crust.